July 1980

WIND POWER CHARGED AEROSOL GENERATOR

FINAL REPORT

Alvin M. Marks

MARKS POLARIZED CORPORATION
153-16 Tenth Avenue
Whitestone, NY 11357

Prepared Under Subcontract No. XH-9-8128-1
for the

SOLAR ENERGY RESEARCH INSTITUTE
A Division of Midwest Research Institute

1536 Cole Boulevard
Golden, Colorado 80401

SERI/TR-XH-9-8128-1
UC Category, UC-60

WIND POWER CHARGED AEROSOL GENERATOR

Draft Final Report

July 1980

Alvin M. Marks

MARKS POLARIZED CORPORATION
153-16 Tenth Avenue
Whitestone, NY 11357

Prepared Under SUBCONTRACT
NO. XH-9-8128-1
FOR THE

SOLAR ENERGY RESEARCH INSTITUTE
A Division of Midwest Research Institute

1536 Cole Boulevard
Golden, Colorado 80401

Printed in the United States of America
Available from:
National Technical Information Service
U. S. Department of Commerce
5285 Port Royal Road
Springfield, VA 22161
Price:
Microfiche $3.00
Printed Copy $6.00

NOTICE

TABLE OF CONTENTS

ABSTRACT

This describes experimental results on a Charged Aerosol Wind/Electric Power Generator, using Induction Electric Charging with a water jet issuing under water pressure from a small diameter (25-100 μm) orifice. The jet breaks into electrically charged water droplets dispersed into the wind stream. New hydraulic and electrical characteristics were obtained. The electro-viscosity effect increases as the orifice diameter decreases. A plate orifice 35 μm diameter, and 25 μm long appears optimum; a single jet from such an orifice at a water pressure of 15 psig produces net electric power output substantially exceeding the hydraulic and electric power inputs. A projection is made for a multi-orifice array as a basis for a practical Generator scaled to a multi-megawatt Wind/Electric Generator. A Water recovery and pressure regeneration means is described by which water is conserved and the water power is free, so that there is a net output electric power without external power input of any kind.

1. BACKGROUND

Our work dates back to the 1940's which culminated in a patent[1], filed on December 14, 1949. In this patent, Figure 12 shows that at 18 m/s a maximum electric power of 3 kW/m^2 would be transduced at a pressure of 1 atmosphere (at 100% efficiency). In a U. S. Patent[2] filed June 23, 1967, this discovery was specifically applied to Wind/Electric Power Conversion[2.1], predicting an electric output power of 1 kW/m^2 (assuming conversion of 33% of the kinetic power of the wind at 17.3 m/s and 33% efficiency). In January 1972, our paper[3] on the same subject was published. On December 30, 1971, we wrote to the Executive Office of the President a letter[4] proposing, among other things, the Wind/Electric Power Generator (WPG). In February 1972, a letter was received from the White House, from Dr. Edward E. David[5], Science Advisor to the President, who stated that both EGD and WPG would be considered.

Subsequently, on October 25, 1973, we made a proposal to the NSF[6] and in 1975 were favored with a grant[7]. Subsequently, we were funded by ERDA[8], and presently by DOE, via SERI[9]. With the exception of other recent work[10], to our knowledge, the only other paper on a Charged Aerosol Wind/Electric Power Generator was a theoretical study published in France[11].

In a letter to President Carter[12] and in recent correspondence[13], we sought a crash program to accelerate work on the WPG.

Under previous ERDA and NSF grants, a wind tunnel test facility was developed and preliminary tests conducted of several electrofluid dynamic (EFD)

aerosol charging devices. Resulting data demonstrated feasibility of the concept. The key technical problem is to develop a method of efficiently charging the aerosol.

The present work provides electrical and hydraulic experimental data on single orifices which enabled a projected scaleup to a multi-megawatt electric power output, with an overall efficiency exceeding 90%.

Several methods were identified in the course of the earlier studies, which could possibly provide for an adequate source of charged droplets. Of these methods, four were investigated:

1. Waterjet/metal contact charging
2. Steam/metal contact charging
3. Condensation ion charging
4. Induction charging/waterjet.

Experimental results from these methods were compared with theories that were derived previously for a range of temperature, humidity and velocity conditions. The results of these studies indicated that the induction charging/waterjet method showed the most potential for providing a source of charged droplets.

The renewal proposal was reviewed by the Special Programs Office, Solar Energy Research Institute (SERI), and the Wind Systems Branch, Department of Energy (DOE), which resulted in a detailed consideration of the tasks proposed. The former effort by Marks Polarized Corporation had been funded under Contract No. EG-77-C-01-2774 with DOE. This effort is funded by the Wind Energy Innovative Systems program at SERI.

2. OBJECTIVE

The objective of the proposed study is to investigate the performance of the Induction Charging/Waterjet technique of producing charged aerosols for a variety of geometries and test conditions and to optimize the performance for standard conditions as detailed in the Scope of Work.

3. APPARATUS AND EXPERIMENTAL PROCEDURE

Method 4.1 previously described[8] utilizes compressed air power input which presently far exceeds the output electric power. This method was chosen to produce the charged aerosol because this method was best known at the time and the charged aerosol was readily controlled. This method, in its present form, is unsuitable for the efficient production of charging aerosols in a practical Wind/Electric Power Generator.

Method 5.1 previously described[8], shown in Figure 1, was developed using water pressure only and electric induction charging from an external electrode of water jets issuing from an orifice in a capillary tube. No heat power or air power is needed. Liquid water at ambient temperatures is employed. The electric power input is much smaller than the electric power output. The charged droplets are produced by the instability of the jet issuing into the air stream and by electrical forces.

Figure 1 shows the experimental setup of the water jet with Induction Electric Charging placed within a wind tunnel as previously described[7,8]

To perform the experiments with orifice tubes of differing lengths, small diameter tubing was obtained, cut to various lengths and mounted in the tubular design shown in Figure 2.

To perform the experiments, it was required to obtain the sizes 2-76 μm diameter with circular orifices in thin sheets. We had been assured by a supplier that they would be able to deliver our requirements; however, after several months had transpired, these orifices arrived but were unsatisfactory because they were over-

sized and the metal had melted forming an irregular rim around the apertures. We were able to locate another source of supply which had stock of aperture sizes 10, 15, 25, 35, 50, and 100 μm. Other apertures were not obtainable. All of these apertures were 25 μm thick (long) in stainless steel sheet discs 9.5 mm diameter, herein termed orifice plates. A special mounting shown in Figure 3 was devised to retain the orifice plates. The thin sheet metal near the orifice is supported between two thicker plates each with a larger diameter hole, to prevent excessive distortion under water pressure.

Since small currents, from 0.01 to 1 μA, and voltages from 1 to 40 kV were to be measured, it was necessary to insulate the emitter (orifice) tube, and the water supply, to minimize electrical leakage.

Figure 4 diagrammatically shows the appearance of the water jet during formation of a charged aerosol using a ring exciter. Figures 5 and 6 show views of a tubular exciter.

The leakage to ground manifested itself as the leakage resistor R' in parallel with the load resistor R. An independent measurement of the values of R and R' was made to assure that the leakage resistance R' was negligible compared to the load resistance R. A difficulty was the occasional clogging of the orifices. This could be cured by reverse flow under water pressure using a special fixture, and by utilizing distilled water, filtered through a fine qualitative grade paper filter and then a fritted glass funnel. This procedure was necessary because commercial distilled water sometimes contains suspended particles. The distilled water was placed in a Plexiglas column to which air was applied from an insulating air column, through an

insulated polypropylene plastic tube. In this manner the Plexiglas reservoir was insulated from ground. The air pressure was measured at the source.

4. EXPERIMENTAL MEASUREMENTS

4.1 Hydraulic Measurements

In making the hydraulic measurements, the flow rate was obtained for each of the orifice diameters, for various values of pressure. This was done by allowing the jet to fill a small container for a given length of time. The container was then weighed on a sensitive balance and the mass volume flow rate thus determined.

The hydraulic power input was then computed from:

$$P_h = P_r Q \tag{1}$$

Since the area is determined from the orifice diameter, the velocity of the jet was then computed from:

$$U = Q/A \tag{2}$$

where

$$A = (\pi/4)\, d_j^2 \tag{3}$$

The kinetic power was then determined from:

$$P_j = (\delta/2)\, U^3 A \tag{4}$$

The hydraulic efficiency then defined is the ratio of the kinetic power of the jet to the input hydraulic power:

$$E_{fh} \equiv P_j/P_h \tag{5}$$

According to conventional theory an orifice in a thin plate should convert about 62% of the hydraulic power to kinetic power of the jet.[16] With the small orifices

25 μm long of 10-100 μm diameter, it was found that hydraulic efficiency decreased with the orifice diameter, and pressure. With orifice diameters of 50 μm or more, the hydraulic efficiency increased with pressure to a maximum of 70%; exceeding the literature value of 62%. With small orifices the apparent viscosity of the water jet increases as the orifice diameter decreases. These characteristics may be ascribed to the electroviscosity effect, which is due to the electrical orientation of the dipolar water molecules in close proximity to the edges of the orifice. The mathematical physics of this effect has been described[14]. Figures 7-10 inclusive summarize our hydraulic observations. Figure 7 shows % Hydraulic Efficiency vs. Water pressure for orifice diameters 25, 35, 50, and 100 μm and orifice plate 25 μm long. Figure 8 shows % Hydraulic Efficiency vs. orifice diameter for various Water Pressures. Figure 9 shows % Hydraulic Efficiencies of tube orifices vs. orifice length in μm for various pressures, for a constant 50 μm orifice diameter. It is apparent that the shorter the length of the orifice the greater the hydraulic efficiency, limited to a maximum efficiency of 62-70% for the given orifice diameter and pressure. It is well known from fluid mechanics[17] that the shorter the pipe the less the pressure drop and hence the greater the hydraulic efficiency, which our tests confirmed. Figure 10 shows Water Jet Velocity vs. Orifice diameter (μm) for a length 25 μm, for various orifice diameters

Figures 7 and 8 show the results of the measurements on 25, 35, 50, and 100 μm orifices of a constant 25 μm length. For the smaller diameter orifices, the hydraulic efficiency increases with increasing pressures. For orifices greater than about 50 μm, this peak efficiency is about 70%, exceeding the maximum 62% efficiency

reported in the literature.[16] The smallest orifice diameter which can be utilized without sacrificing peak efficiency is about 50 μm; for the best combination of hydraulic and electrical characteristics, 35 μm is preferred.

As the orifice diameters decrease to less than 35 μm, the electroviscosity effect greatly increases, and the hydraulic efficiency rapidly decreases. We were able to obtain well defined jets from orifices as small as 25 μm, but were not successful in producing jets from orifices 15 μm or less. The reason for this may be understood from Figure 8, which shows that the hydraulic efficiency rapidly approached zero for orifices smaller than about 22 μm.

4.2 Electrical Measurements

Electrical measurements typically involved measuring the generated voltage on the emitter V_1, the emitter or charged aerosol current I_1, and the load resistance R. The input electrical quantities were the exciter/emitter potential difference V_2 and the exciter current I_2. From these values, the output electrical power was calculated:

$$P_{eo} = I_1 V_1 \qquad (6)$$

and the input electrical power was calculated:

$$P_{ei} = I_2 V_2 \qquad (7)$$

The total input power comprises the electrical power input P_{ei} and the hydraulic power input:

$$P_{in} = P_{ei} + P_h \qquad (8)$$

These quantities are correlated by plotting experimental values of power versus water pressure on the log-log graphs Figures 11 through 17 for various orifice diameters and lengths.

4.3 System Measurements

In evaluating the system both hydraulic and electrical measurements must be considered. Figures 11-18 are log-log graphs on the same scale for easy comparison, in which the ordinates are shown as the logs of the power inputs and outputs and the abscissae are the logs of the water pressure. These plot as approximately straight lines showing that they are power functions. In accordance with theory, the hydraulic power and the jet kinetic power both plot approximately as $P_r^{3/2}$. For orifices less than 50 μm long, the electrical measurements of the power output plot according to $P_r^{1/2}$. The electrical power output exceeds the hydraulic power output at small water pressures.

The most important characteristics of these curves is the breakeven point, where $P_{eo} = P_h$, and the value of the power at this point.

At this point the slope of P_h is always nearly 3/2 for a 25 and 50 μm thickness.

It is emphasized that the measurements made herein were on single orifices only. For small diameter orifices, the outputs were from 0.05 to 0.5 μA, and the output voltages from 3 to 32 kV. An important quantity is φ. The charge density φ increased as the orifice diameter decreased. This relationship is shown in Figure 22, in which the values of φ are plotted as ordinates vs. the water Pressure P_r in psig as abscissae for orifice diameters of 25, 35, and 50 μm.

TABLE NO. 1

RESULTS OF ELECTRICAL AND HYDRAULIC MEASUREMENTS ON BREAKEVEN POINT VALUES

Figure No.	Orifice		Breakeven Power Point	Water Pressure	Slope	Comments
	Dia d_j	Length L_o	$P_{eo} = P_h$	P_r	$\Delta P_{eo}/\Delta P_r$	
	μm	μm	Watts	psig	watts/psig	
11	76	2000	5×10^{-5}	1		
12	50	2000	$< 10^{-5}$	< 1	about 1.3	
13	50	1000	$< 10^{-5}$	< 1	about 1.3	
14	74x110	50	4×10^{-4}	4.5	about 0.5	
15	50	25	1.3×10^{-4}	2.2	about 0.5	First breakeven
15	50	25	4.5×10^{-2}	105	about 10	Second breakeven
16	35	25	8.5×10^{-4}	17	about 0.5	
17	25	25	8×10^{-5}	10	about 0.5	
18	35	25	3×10^{-1}	200	about 0.5	Projected Values 3x3 array = 9 orifices

The table shows that results for the 35 μm plate orifice 25 μm long have the best characteristics; that is, the greatest electric power output, at the breakeven point, at a suitably large operating pressure of 16 psig.

The characteristics shown in Figure 16 for the 35 μm orifice 25 μm long, compared to the characteristics shown in Figure 17 for a 25 μm orifice, 25 μm long, show that the former is the optimum since in the latter the breakeven power is decreased for the 25 μm diameter by about 9 times, and the breakeven pressure is decreased from 17 to 10 psig.

Hence, 35 μm diameter, 25 μm long appears to be optimum. On the last line of Table 1 the projection of the results from Figure 16 are plotted on Figure 18 for n_a = 3x3 = 9 multi-orifice array. At a constant load resistance, the electric power increases according to n_a^2 = 81 times; for the hydraulic power increases according to n_a = 9 times.

For example, at P_r = 25 psig P_{eo} = 0.1 watt, and P_h = 0.015 watt. Thus, in this example, the ratio of output electric power to input hydraulic power is:

$$P_{eo}/P_h = 0.1/0.015 = 6.7 \text{ times}$$

This scaling is projected ultimately to the multi-megawatt range in Figure 34, using the same 35 μm orifices 25 μm long and operating in the same pressure range as in Figure 16; to be discussed hereinafter in connection with the proposed engineering designs shown in Figures 28 and 29.

The Figure 15 shows a new interesting and important characteristic: an apparent second breakeven point projected to be at about 200 psig and 4.5×10^{-2} watts, compared to 1.3×10^{-4} watts at 2.2 psig; a ratio of about 300 times greater

electric/hydraulic power, and the electrical power rising rapidly with a slope of about 10, compared to the hydraulic power slope of 1.5. This must be investigated.

4.3.1 Effect of Varying Exciter–Emitter Voltage V_2

Figure 19 shows output current I_1 in μA and output voltage V_1 in kV vs. Exciter Voltage V_2 at various water pressures P_r in psig for a plate orifice 25 μm diameter, and 25 μm long.

An important result is that the output current I_1 is independent of the exciter voltage V_2 up to a maximum value which increases with the water pressure P_r. Thus $\bar{I}_1$ = .04 μA with P_r = 40 psig at V_2 = 6 kV, but $\bar{I}_1$ = .045 at 50 psig and V_2 = 8kV. The same is true of the output voltage, but the slope $\Delta V_1/\Delta V_2$ varies.

Figure 20 shows the results of tests made on a 50 μm diameter orifice plate 25 μm long, varying voltage V_2 on output voltage and input and output currents and constant water pressure P_5 = 50 psig. The output voltage and current increase approximately linearly with V_2 up to a critical voltage, after which the exciter current and output current increased rapidly. With a further increase in V_2 the output voltage becomes unstable and starts to decrease because the exciter is then drawing excessive power away from the jet.

Figure 21 shows output current I_1, and input current I_2 μA and output V_1 and input V_2 voltages kV vs. a water pressure P_r in psig such that $I_1 = I_2$ for a plate orifice 50 μm diameter and 25 μm long. The exciter–emitter voltage V_2 may be increased linearly with the pressure until $I_1 = I_2$; I_1 and I_2 increase linearly with V_2 after an initial rapid rise; but as $P_r > 60$ psig and V_2 increases beyond 8 kV, I_1 and I_2 rapidly increase producing an increase in φ from about 1.5 to about 4, and

the output voltage also increases; but apparently linearly instead of faster as might be expected. This effect deserves more experimental study.

An important characteristic of the system is the charge per unit volume of water which is defined:

$$\varphi \equiv I_1/Q \tag{9}$$

4.3.2 Ring Exciter Diameter and Position

The water jet was subjected to an electric field from an exciter electrode. Various tests were made to determine the best value of exciter ring diameter and position relative to the plane of the orifice. The best results were obtained with an exciter diameter of about:

$$d_{ex} = 60 \text{ mm}$$

placed about 10 mm in front of the orifice plane, and most of the tests were taken with these values.

During the first 11 months of the contract, work was performed with the exciter in the form of a ring electrode as shown in Figure 1.

4.3.3 Tubular Exciter Diameter Length and Position

A mathematical physical formulation was sought in which φ was derived on first principles. A formula was found in a reference[15] relating to the charge on a coaxial condenser; equation (58). Using this formula, which assumes that the charge resides on the surface of the jet which is considered to be the inner coaxial cylinder of the condenser, a formula was derived for φ as a function of the various physical quantities involved; see equation (61).

This formula suggested that an exciter in the form of a cylinder rather than a

ring would produce a greater output current. In the time available, we performed a number of experiments which prove this to be indeed the case. In these recent experiments, with the tubular exciter, certain practical difficulties were encountered, particularly to align the jet along the axis of a long narrow tube. Accuracy of the alignment of the jet on the axis of the cylinder is critical to the optimum functioning of this system. Redesign and further test of the emitter–tubular exciter structure is indicated. These were made using exciter tubes of various lengths and diameters which theory indicated should show increased output electric currents compared with the ring exciter, and this effect was observed, as shown in Figures 30 and 31.

A further interesting result was obtained in these experiments: the measured value of φ was about 30 times greater than the calculated value of φ. This may be ascribed to the breakup of the jet into many smaller cylinders or filaments, each of which have a greater current-carrying capacity than a whold jet of greater diameter. Figure 4 shows the appearance of a jet in an electric field just prior to its spraying to form a charged aerosol. The jet appears to thicken. This supports the theory of the jet expanding to form parallel filaments of water.

The extraordinarily improved results were obtained with a plate orifice 100 μm diameter and 25 μm long, and a tubular exciter.

It is now necessary to repeat these tests with a plate orifice 35 μm in diameter and 25 μm long, again taking the electrical and hydraulic measurements using a tubular exciter of optimum dimensions, which should provide greatly improved system characteristics. The existing measurements have enabled the design of a multiple orifice array as shown in Figures 28 and 29.

4.4 Atmospheric Wind/Electric Power Transduction

The results of the experiments performed in the wind tunnel using Method 4.1 under various operating conditions are given in Figures 32 and 33. At relative humidities of 25 to 95%, air temperatures of 20 to 40°C, and velocities of from 2.5 to 16 m/s, an electric efficiency of 75 to 97% is obtainable.

5. MATHEMATICAL PHYSICS

5.0 Table of Symbols

A	Area of orifice, or jet		m^2
b	Breakdown strength, air, S.T.P. = 3×10^6		V/m
C	Capacitance		farads
d_{ex}	Diameter of exciter ring or tube		m, μm
d_j	Diameter of orifice		m, μm
E_b	Breakdown electric field intensity		V/m
E_{fe}	Electric efficiency		%
E_{fh}	Hydraulic efficiency		%
E_{fo}	Overall efficiency		%
$f(x)$	Function of $x = x/\ln x$		
F_m	Figure of Merit	$10^6\ I/P_{in}$	μA/watt
i_1	P_{eo}/V_1		amps, μA
I_1	Load current		amps, μA
I_2	Exciter current		amps, μA
k_a	Charged aerosol breakdown factor ≈ 1		
k_o	$1.176 \times 10^{23}/d_j$ Equation (25)		μm
$k_1 \equiv$	$(0.68/k_o)^{\frac{1}{2}}$ Equation (27)		
$k_2 \equiv$	$(1 + P_{ei}/P_h)$		
L_e	Distance of exciter electrode from orifice plane		m
L_o	Length of Tubular exciter electrode parallel to jet		m
N	Number of electrons on charged droplet		
n_a	Number of sources		
n_1	Number of orifice sources per unit area		
p_e	Electric output power density		W/m^2
P_{ei}	Input electric power		W
P_{eo}	Output electric power		W
P_h	Input hydraulic power		W
P_{in}	Total input power		W
P_j	Jet kinetic power		W
P_{ri}	Total hydraulic pressure drop		psi
P_{rj}	Hydraulic pressure drop to produce jet only		psi
P_r	Water Pressure		psig
q	Electric charge		c
Q	Water flow rate of jet issuing from an orifice		m^3/s
Q_1	Flow rate of water per unit area (same as velocity)		$m^3/s\text{-}m^2$ or m/s
r_o	Radius of isolated sphere		m
r	Radius of droplet		m, Å
R	Resistance of load		ohms
R_{oi}	Ratio of electric power-out to total power-in		
T	Air temperature absolute		°K
U	Wind velocity		m/s
U_w	Water velocity		m/s
V_1	Load voltage		kV

5.0 Table of Symbols (Continued)

V_2	Emitter exciter potential difference	kV
V_E	Exciter jet potential difference	kV
v_o	Fictitious voltage drop representing all losses	kV
ϵ_o	Dielectric constant of free space 8.854×10^{-12}	farads/m
η	$\epsilon_o (bk_a)^2/2 = 40$	N/m^2
φ	Electric charge per unit volume of droplet	c/m^3
ρ_w	Density of liquid water	kg/m^3
Δ	Change	
$'$	Ideal	
$\bar{}$	Maximum value of symbol	

5.1 Hydraulic Relationships

$$P_h = P_r Q \quad (10)$$

$$P_j = (\delta/2)\, U^3 A \quad (11)$$

$$Q = AU \quad (12)$$

$$P_j = (\delta/2)\, Q^3/A^2 \quad (13)$$

E_{fh} = the ratio < 1

$$E_{fh} \equiv P_j/P_h = (\delta/2)\, Q^3/A^2 P_r Q = (\delta/2)\, (Q/A)^2/P_r \quad (14)$$

$$E_{fh} = (P_r'/P_r) \qquad \text{where } P_r' \equiv (\delta/2)\, U^2 \quad (15)$$

$$E_{fh} = (\delta/2)(4/\pi)^2\, Q^2/P_r d_j^4 \quad (16)$$

Using MKS units

Q in m^3/s

P_r in n/m^2

d_j in m

$(\delta/2)$ = 500 for water

$$E_{fh} = 811\, Q^2/P_r\, d_j^4 \quad (17)$$

Expressing these useful units:

Q in m^3/s

P_r in psig x 6895 = n/m^2

d_j in $\mu m \times 10^{-6}$ = m

$$E_{fh} = \{500(4/\pi)^2 (1/6895)(10^{-6})^4\}\, [Q^2/P_r d_j^4] \quad (18)$$

$$E_{fh} = [5\, (4/\pi)^2\, (1/0.6895)]\, (10^2/10^{4-24})\, (Q^2/P_r d_j^4) \quad (19)$$

$$E_{fh} = 11.76 \times 10^{22}\, (Q^2/P_r d_j^4) \quad (20)$$

$$E_{fh} = 1.176 \times 10^{23}\, (Q^2/P_r d_j^4) \quad (21)$$

E_{fh} is usually ≈ 0.68 $k \equiv 1.176 \times 10^{23}$

For this condition:

$$Q = (E_{fh}/k)^{1/2} P_r^{1/2} d_j^2 \quad (22)$$

$$= (0.68/1.176 \times 10^{23})^{1/2} P_r^{1/2} d_j^2 \quad (23)$$

$$Q = 2.40 \times 10^{-12} P_r^{1/2} d_j^2 \quad (24)$$

The simplest approach to computing orifice efficiencies is to calculate for each orifice diameter 15, 25, 35, 50, 76, 100, and 300 μm values of k_o;

$$k_o \equiv (1.176 \times 10^{23}/d_j^4) \quad (25)$$

in which d_j is expressed in μm (see equation (21)).

$$E_{fh} = k_o (Q^2/P_r) \quad (26)$$

hence knowing the flow rate Q in m^3/s and P_r in psig, the efficiency is quickly calculated for each orifice diameter.

It was found that for $d_j \geq 50$ μm and $P_r > 10$ psig

E_{fh} = 0.68; for which

$$Q = (0.68/k_o)^{1/2} P_r^{1/2} = k_1 P_r^{1/2} (m^3/s) \quad (27)$$

For smaller orifice diameters and pressures the electro-viscous effect causes the % hydraulic efficiency to decrease and its value can be determined experimentally from (26). Table of values of k_o and k_1 vs. d_j follows:

d_j (μm)	k_o	k_1
15	2.32×10^{18}	5.41×10^{-10}
25	3.01×10^{17}	1.50×10^{-9}
35	7.84×10^{16}	2.95×10^{-9}
50	1.88×10^{16}	6.01×10^{-9}
76	3.52×10^{15}	1.39×10^{-8}
100	1.18×10^{15}	2.40×10^{-8}
300	1.45×10^{13}	2.16×10^{-7}

5.2 Hydraulic-Electric Relationships

5.2.1 Ratio of Output to Input Power at Constant Generated Voltage $\tilde{V}_1$

The resistance R is varied to maintain the output at a constant voltage $\tilde{V}_1$. For example, if $\tilde{V}_1 = 10^5$ and if V_2 is adjusted to obtain a maximum E_b; then:

$$P_{eo} = I_1 \tilde{V}_1 = \varphi Q \tilde{V}_1 \qquad (28)$$

but where P_{eo} is the wind/electric power output:

$$P_h = P_r Q \qquad (29)$$

Hence from (28) and (29), R_{oi} takes on this simple form:

$$R_{oi} \equiv P_{eo}/P_h = \varphi Q \tilde{V}_1/P_r Q \qquad (30)$$

$$R_{oi} = \varphi \tilde{V}_1/P_r \qquad (31)$$

EXAMPLE 1

Given:

$\varphi = 3$ c/m^3

$\tilde{V}_1 = 10^5$ volts

$P_r = 7 \times 10^4$ (10.12 psig)

Find:

R_{oi}

From (31):

$$R_{oi} = 3 \times 10^5/7 \times 10^4 \approx 4.3$$

The output power is 4.3 times the input power.

In equation (31) since R_{oi} is a dimensionless ratio, it is apparent P_r/φ has the dimensions of a fictitious equivalent voltage V_o:

$$V_o \equiv P_r/\varphi. \qquad (32)$$

and hence:

$$R_{oi} = V_1/V_o \quad (33)$$

For example, in a useful Wind/Electric Power Generator, the ratio of output wind/electric power, to input power (electric, hydraulic) would be $R_{oi} \geq 10$.

The Figure of Merit F_m previously defined[1] is then:

$$F_m \equiv 10^6/V_o = 10^6 \varphi/P_r \quad (34)$$

The fictitious voltage V_o is that equivalent voltage which would be required to provide the aerosol current I_1 with an input electrical power equal to the input hydraulic power; that is:

$$I_1 V_o \equiv P_r Q = P_h \quad (35)$$

$$V_o \equiv P_r/(I_1/Q) = P_r/\varphi \quad (36)$$

The equation (35) may be modified to include the input electrical power to the exciter, $P_{ei} = I_2 V_2$

Then

$$I_1 V_o' \equiv P_r Q + I_2 V_2 \quad (37)$$

$$V_o' = (P_r/\varphi) + (I_2/I_1) V_2 \quad (38)$$

$$V_o' = V_o [1 + (I_2 V_2/I_1 V_o)] \quad (39)$$

$$V_o' = V_o [1 + (P_{ei}/P_h)] = k_2 V_o \quad (40)$$

If V_2 is regulated to keep I_2 small, then $P_{ei}/P_h \ll 1$ $k_2 \rightarrow 1$ and

$$V_o = V' \quad (41)$$

where $k_2 \equiv (1 + P_{ei}/P_h)$

It will be assumed that the input electric power is a small fraction of the output wind/electric power and that the water power is the main input power.

EXAMPLE 2

For a 25 μm diameter orifice in a 25 μm thick plate, the measured value of φ = 10 at a water pressure P_r = 40 psig = 40 x 6895 = 2.76×10^5 n/m^2.

Given:

V_1 = 100 kV for multiple orifices

Find:

(1) V_o

(2) F_m

(3) R_{oi}

V_o = 40 x 6895/10 = 27580 volts (fictional)

F_m = $10^6/V_o$ = 10^6/27580 = 36.3 μA/Watt

R_{oi} = 100,000/27580 = 36.3

at 10 psig R_{oi} = 14.5

that is input water power is only 8% of the output wind/electric power.

EXAMPLE 3

Given:

d_j = 25 μm

φ = 10 c/m^3

V_1 = 10^5 volts

R_{oi} = 10

Find:

(1) P_r

(2) V_o

(3) F_m

Answer:

(1) From (31):

$$R_{oi} = \varphi V_1/P_r = 10 \times 10^5/P_r$$

$$P_r = 10^5 \text{ n/m}^2 \approx 14 \text{ psig}$$

(2) from (36): $V_o = P_r/\varphi = 10^5/10 = 10^4 \text{ v} = 10 \text{ kV}$

(3) from (34): $F_m = 10^6/V_o = 10^6/10^4 = 100$

Find the Output Current I_1 in terms of P_r, d_j, φ:

From (9) and (24):

For Q in m^3/s; P_r in psig; and d_j in μm:

$$I_1 = \varphi Q = 2.39 \times 10^{-12} P_r^{\frac{1}{2}} d_j^{\frac{1}{2}} \varphi \qquad (42)$$

EXAMPLE 4

Given:

φ = 10

d_j = 25 μm

P_r = 20 psig

Find: I_1 in μA

From (42):

$$I_1 = 2.39 \times 10^{-12} (20)^{\frac{1}{2}} (25)^2 10$$

$$I_1 = 0.0668\ \mu A$$

5.2.2 Electrical Output Power per Orifice

$$P_{eo} = I_1^2 R = (2.39 \times 10^{-12})^2 R P_r d_j^4 \varphi^2 \quad (43)$$

$$P_{eo} = 5.71 \times 10^{-24} R P_r d_j^4 \varphi^2 \quad (44)$$

From (31):

$$P_r = \varphi (V_1/R_{oi}) \quad (45)$$

From (44) and (45), eliminating P_r:

$$P_{eo} = 5.71 \times 10^{-24} R (V_1/R_{oi}) d_j^4 \varphi^3 \quad (46)$$

5.2.3 Empirical Equation of φ vs. P_r

From Figure 22 for the special case where $d_j = 25\ \mu m$ the relationship is a straight line with this equation for P_r in psig:

$$\varphi = 14.9 - 0.111 P_r \quad (47)$$

From (34):

$$P_r = 10^6 \varphi / F_m \quad (48)$$

EXAMPLE 5

Given:

$d_j = 25\ \mu m$

$L_o = 25\ \mu m$ (Length of orifice)

$F_m = 100\ \mu A$

$V_1 = 10^5$ volts

Find:

(1) P_r in psig

(2) φ

(3) R_{oi}

From (48) putting $F_m = 100\ \mu A/watt$, and dividing by 6895 to put P_r in psig:

$$P_r = 1.45\,\varphi \tag{49}$$

Solving (47) and (49) simultaneously:

$$(P_r/1.45) + 0.111\ P_r = 14.9 \tag{50}$$

$$0.800\ P_r = 14.9 \tag{51}$$

(1) $$P_r = 18.62 \text{ psig} \tag{52}$$

(2) $$\varphi = 12.8 \tag{53}$$

(3) From (31):

$$R_{oi} = 10^5 \times 12.8/18/6 \times 1895 \approx 10 \tag{54}$$

Figure 23 shows experimental values of the Figure of Merit F_m vs. Water Pressure P_r psig for plate orifices having 25, 35, and 50 μm diameters for a constant length 50 μm. Values of $F_m \geq 100$ are obtained with 25 μm and 35 μm orifices. There is a projection at pressure > 70 psig for a 50 μm diameter orifice which shows that it may be possible to obtain $F_m > 100\ \mu A/Watt$ in this range. This must be further investigated.

Figure 25 shows Input and Output Currents and Input and Output Voltages vs. Load Resistance ohms for various conditions. There is an optimum resistance $R \approx 10^{11}$ ohms for 25 and 35 μm single orifices, at which the output electric power P_{eo} is a maximum. At greater resistances $R \rightarrow R'$ the leakage resistance, and power is lost.

5.2.4 Induction Charging of a Water Jet

The water flow rate Q of the jet is:

$$Q = (\pi/4)\, d_j^2\, U \tag{55}$$

The current flow rate is:

$$I_1 = q\, U \tag{56}$$

Then by (55) and (56):

$$\varphi \equiv I/Q = q/(\pi/4)\, d_j^2 \tag{57}$$

Referring to Figures 5 and 6; if it is assumed that the:

(1) Current is carried by the circumference of the jet

(2) Surface charge density is the same as corresponding coaxial cylinders.

Then, the capacitance of the 2 coaxial cylinders (exciter tube and jet) in mks units is:[15]

$$C = 4\pi\, \epsilon_o\, L_e/2 \log (d_{ex}/d_j) = 2\, \pi\, \epsilon_o\, L_e/\ln (d_{ex}/d_j) \tag{58}$$

$$q = V_2\, C = 2\, \pi\, \epsilon_o\, V_2\, L_e/\ln (d_{ex}/d_j) \tag{59}$$

Hence from (57) and (59):

$$\varphi = 8\, \epsilon_o\, V_2\, L_e/d_j^2 \ln (d_{ex}/d_j) \tag{60}$$

For V_2 volts, L_e in m, d_{ex} and d_j in μm

$$\varphi = 70.83\, V_2\, L_e/d_j^2 \ln (d_{ex}/d_j) \tag{61}$$

EXAMPLE 6

V_2 = 5×10^3 volts

L_e = 2×10^{-2} m

d_j = 100 μm

d_{ex} = 3 mm (3000 μm)

Find: φ

From (61):

$\varphi = 70.83 \times 5 \times 10^3 \times 2 \times 10^{-2}/(10^2)^2 \ln (3000/100)$

$\varphi = (70.83/8.82) \times 10^{-2}$

$\varphi = 8.03 \times 10^{-2}$

EXAMPLE 7

Given: The same conditions as Example No. 6

Find: φ for various values of d_j.

Answer: See Table 2 and Figure 24.

TABLE 2

φ, the electric charge per unit volume of water VS d_j, diameter of the water jet for d_{ex} = 3 mm and L_e = 20 mm	
d_j in μm	φ in c/m^3 (calculated)
1	885
5	59
10	12
15	6
20	3.5
35	1.3
50	0.7
75	0.34
100	0.08

Values of $\varphi \approx 3\text{-}10$ are observed, for $d_j = 100$ and $25\ \mu m$, respectively.

The apparent discrepancy between φ_{obs} and φ_{calc} can be explained if the charge is considered confined to many smaller diameter jets, or to discrete charged droplets. This causes $x = d_{ex}/d_j$ and $f(x)$ to increase, and φ is increased to the observed value.

The maximum exciter voltage V_2 is limited by spark breakdown or excessive exciter current, and this limits the maximum attainable value of φ:

Since V_2 is the voltage across a radius = $d_{ex}/2$ and $d_j \ll d_{ex}$:

$$\varphi = 70.8\ L_e\ [V_2/(d_{ex}/2)]\ (d_{ex}/2d_j)/d_j\ \ln\ (d_{ex}/d_j) \quad (62)$$

At atmospheric pressure the breakdown electric field per μm is:

$$E_b \leq 3\ v/\mu m \text{ or } 3 \times 10^6\ v/m$$

$$2(V_2/d_{ex}) \leq E_b = 3 \times 10^6\ v/m = 3\ v/\mu m \quad (63)$$

Define:

$$(d_{ex}/d_j) \equiv x \quad (64)$$

$$f(x) \equiv x/\ln x \quad (65)$$

From (61)(63)(64) and (65); expressing d_j in μm; and E_b in $v/\mu m$

$$\varphi = 35.4\ E_b \cdot L_e\ (1/d_j)\ f(x) \quad (66)$$

5.2.5 Number of Orifices per Unit Area

$$i_1 = n_1\ I_1 \quad (67)$$

$$Q_1 = n_1\ Q \quad (68)$$

$$\varphi \equiv i_1/Q_1 = I_1/Q \quad \text{charge density on water droplets } c/m^3 \quad (69)$$

To find the flow rate per unit are:

$$Q_1 = i_1/\varphi = n_1\ I_1/\varphi = n_1\ Q \quad (70)$$

$$i_1 = P_{eo}/V_1 \quad (71)$$

EXAMPLE 8

Given:

φ = 10

P_{eo} = 400 Watts/m^2 in a 10 m/s wind

V_1 = 10^5 volts, 10^6 volts

I_1 = 0.1 μA

i_1 = $4 \times 10^2/10^5 = 4 \times 10^{-3}$ amps (4 milliamps)

Find:

(1) Q_1 for $V_1 = 10^5, 10^6$ volts

(2) n_1

From (70):

Q_1 = $i_1/\varphi = 4 \times 10^{-3}/10 - 4 \times 10^{-4}$ $m^3/s\text{-}m^2$

$3600 \times 4 \times 10^{-4} = 1.44$ $m^3/hr\text{-}m^2$

(1) 1 gal = 0.003785 m^3

Q_1 = $1.44/.3785 \times 10^{-2}$ = 380 gph/m^2 for $V_1 = 10^5$ volts

Q_1 = 38 gph/m^2 for 10^6 volts

(2) n_1 = $i_1/I_1 = 4 \times 10^{-3}/0.1 \times 10^{-6}$ = 40,000 orifices

Recovery and recirculation of the water, and pressure regeneration may be used as described in Section 6.2.

EXAMPLE 9

Given: The current I_1 per orifice = 8×10^{-8} amps.

An electric power output = 400 watts in a 10 m/s wind at 10^5 volts

Find: (1) How many amps of current and (2) how many orifices n_1/m^2 are required.

Answer:

i_1 = $400/10^5 = 4 \times 10^{-3}$ amps/m^2 (4 milliamps/m^2)

n_1 = $(i_1/I_1) = 4 \times 10^{-3}/8 \times 10^{-8} = 0.5 \times 10^{-5} = 5 \times 10^4$

n_1 = 50,000 orifices/m^2

It appears advantageous to nave fewer arrays per unit area, and a greater number of orifices per array.

In Figure 29, there is snown a design for a superarray of 36,000 orifices each 35 μm in diameter, and comprising a 6x6 = 36 array of 1024 orifices, each array being 3.5 x 3.5 mm as shown in Figure 28.

5.2.6 Scaleup to Multimegawatt Electric Power Output

Figure 16 shows the output and input electric power and the input hydraulic power for a plate orifice 35 μm diameter, 25 μm long. At a water pressure of P_r = 20 psig, the electric power output P_{eo} = 1 mW at 10^4 volts; the hydraulic power input P_h = 1.3 mW; and the electric power input is about 0.05 mW.

The number of orifices n_a required to increase the output voltage V_1 from the observed 10^4 volts to 1.12×10^6 volts is $n_a = 1.12 \times 10^6/10^4 = 112$ orifices.

For an orifice plate having 112 multiorifices: 112×10^4 volts = 1.12×10^6 volts, at a water pressure of P_r = 20 psig. To generate 400 watts/m^2, there is required 3.6×10^{-3} amps/m^2. Since each orifice emits 0.1 μA = 10^{-7} amps, there are required $(3.6 \times 10^{-3}/10^{-7})$ = 36,000 orifices per m^2 for a 6x6 = 36 superarray /m^2 of multi-orifice arrays, each having 1024 orifices in a 32x32 array. For 10^5 m^2, the electric power output is then: 400×10^5 = 40 megawatts.

The output and input powers per unit area are scaled:

hydraulic power input	=	$n_a P_j$
electric power input	=	$n_a P_{ei}$
electric power output	=	$n_a^2 P_{eo}$

as the exciter-emitter voltage remains constant with the number of orifices.

Hence, at P_r = 20 psig, these are the scaled values for 10^5 m^2 in which 400 W/m^2 is generated in a 10 m/s wind[7.1] :

$V_1 = 1.12 \times 10^6$ volts

$V_2 = 10^4$ volts

$I_1 = 4 \times 10^{-3} \times 10^5 = 400$ amps

$I_2 = 2 \times 10^{-4} \times 10^5 = 20$ amps

Total Output Electric Power:

$$P_{eo} = V_1 I_1 = 1.12 \times 10^6 \times 4 \times 10^2 = 45 \times 10^6 \text{ w} = 45 \text{ Mw}$$

Total Input Electric Power:

$$P_{ei} = 10^4 \times 20 = 2 \times 10^5 \text{ w} = 0.2 \text{ Mw}$$

Total Hydraulic Power Input:

$$P_h = 1.03 \times 10^{-3} \times 3.6 \times 10^4 \times 10^5 = 1.03 \text{ Mw}$$

Total Power Input $(P_h + P_{ei}) = 1.03 + 0.2 = 1.23$ Mw

In this example, the ratio of output to input power is:

$$R_{oi} = 45/1.23 = 33.6 \text{ times.}$$

6. DISCUSSION

6.1 The Tubular Exciter

In the present work the hydraulic relationships were determined experimentally. The relationships and magnitudes of the electrical variables are now known. The

electrical characteristics of the induction charging of single jets have been determined by numerous experiments. Since the advantages of the tubular exciter were discovered late in this contract period, the electrical output power measured using a ring exciter rather than a tubular exciter may be an order of magnitude too small.

A breakthrough discovery was made in increasing the ratio φ which is fundamental to improving the output/irput power ratio R_{oi}.

A formula for the capacitance of coaxial cylinders, modified for the mks system, was applied to the combination of a water jet and a coaxial tube of length L_e. The water jet was considered as the inner "cylinder".

Previously a narrow ring was used as the exciter electrode. For the ring L_e was small, only about 3 mm = 3×10^{-3} m. The jet current and the φ value was found to increase by increasing the capacitance. This was accomplished by increasing L_e and decreasing d_{ex}. Decreasing L_o also increased φ. See Figures 30 and 31.

When the jet extends outward a long distance, viscous forces slow the jet and cause it to expand in cross section. Electrical forces also cause the jet to expand and break apart.

For a 100 μm diameter orifice the calculated value of $\varphi_c = 0.08$ c/m^3 (Table 2) which is 37 times smaller than the observed value $\varphi_o = 3$ c/m^3. Figure 22 shows that this value is obtained for a jet diameter of < 50 μm. The explanation for this discrepancy may be that the charge must be carried by many jet filaments, or droplets of smaller diameter.

The exciter tube not only acts as the outer cylinder of a coaxial condenser, but also as a shield for the space charge produced by the presence of charges along the

jet, preventing the buildup of a back voltage which would limit the current flow along the axis of the jet.

It was observed that φ increases as d_j decreases, everything else being constant.

Figures 28 and 29 show a superarray of multi-orifice jet arrays. A tubular exciter tube may be supported by insulators and spaced from an emitter tube containing the orifice array. This module is shown in Figure 29. The emitter assembly comprises an emitter tube 100 containing the orifice array shown in Figure 28, the tubular exciters 101 and the stand-off insulators 102. A superarray of 36 units mounted in a 1 m^2 module 103 will have 36,000 orifices/m^2, which at 0.1 μA/orifice, will produce a charged aerosol having 3.6 mA/m^2. At 1.12×10^6 volts (400 watts) or 0.4 kW/m^2 electric power output will be generated in a 10 m/s wind. The input water power would be 40 watts and the water flow based on $\varphi = 10$ will be about 38 gph/m^2.

6.2 Water Recuperation and Pressure Regeneration

An optional feature which may be included with this structure is a grounded collector electrode to discharge the charged aerosol and consolidate the water droplets, and cause the water to gather in a container. This water is then pumped by a small pump which utilizes 60 watts input to provide 40 watts hydraulic power to actuate the micro jets. The electrical losses are below 10% because the voltage applied between the exciter and the jet is maintained sufficiently small so that the input power is very much less than the output power. The advantage of the removal of the charged aerosol as water at the collector electrode is that the water must be pumped through a maximum of only 1 m height against gravity, which requires about only 1.2 psig (10^4 n/m^2) plus the water pressure $P_r \approx 20$ psig.

This structure is shown in Figure 27.1.

The collector method has the further advantage of minimizing the use of water since most of it will be recirculated within the system. Figures 27.1 - 27.3 show various water recuperation and pressure regeneration schemes.

Figure 27.1 shows a natural water recuperation and pressure regeneration scheme, in which 200 is a large area wind/electric power generator suspended from a cable 201, supported by towers 202 and feeding high voltage DC electric power via wires 203. The wind 204 carries the charged water droplets 205 to any distance where they discharge on the ground at 206. They may serve to irrigate a large area of land; on which crops may be grown; thus serving a dual purpose. Water evaporates as vapor 207 due to sunlight 208, and the water 209 eventually precipitates on a higher level body of water such as a lake 210. Water is withdrawn from the lake 210 via the pipe 211. Excess water power may be converted to electricity 212 by hydro-electric means 213; and the required remaining pressure, delivered via pipe 214 to the wind/electric power generator screen 200.

In Figure 27.2 a water recuperation collector screen is provided to collect most of the water in the wind stream by attracting most of the charged droplets to grounded collector plates where they drop off into a gutter, and are pumped at the required pressure (perhaps 20 psig). The loss of head due to the height of the collector electrode may be only 1 psig. In the Figure, 217 is a multi-orifice emitter source of charged aerosol 218, the tubular exciter element is 219 and 215 is the grounded collector plates which collect electric charge, and the water. Since the air contains only a comparatively small volume of water vapor at 20-100% saturation (see Table 2 and the volume of charged aerosol water is greater, most of the water will be re-

covered for circulation.

In Figure 27.3 there is shown a water recuperation and pressure regeneration scheme in which the wind stream is redirected vertically by the barrier wall 220. The emitter screen 221 is supported horizontally and the water jets 223 are directed vertically upward. The barrier wall 224 shields the upwardly directed wind stream 225, in which the charged aerosol water droplets 226 are entrained. These charged water droplets are carried vertically upward by the wind stream to a height of about 15 m, where they are collected by the grounded electrode 227, and drip into the gutters 228, where the water collects and returns via the pipe 229 to supply water under a pressure of about 21.7 psig to the water jets. Thus the wind supplies the energy to lift the charged water droplets against the gravitational field, thus converting the wind power to hydraulic power. Simultaneously, the wind power also moves the charged water droplets against the electric field and is converted to output electric power. In this case the hydraulic power input is free.

6.3 Charge Density φ

The charge density φ is increased by decreasing d_j, by using a tubular exciter, and by using a maximum exciter voltage V_2.

Greater currents and φ values are achieved by increasing the exciter tube length to an optimum length (about 50 mm); decreasing its diameter (to about 3 mm); and placing it close to the jet orifice (about 5 mm).

A practical problem is the centering of the jet along the exciter tube axis, but this only requires a more accurate mounting, and better support for the thin orifice plate.

6.4 Self-Limiting Exciter Current due to Space Charge

Referring to Figure 25, it is observed that as R is increased V_1 increases, I_1 decreases P_{eo} is approximately constant V_2 is constant I_2 decreases for no apparent reason since V_2 is constant. I_2 and P_{ei} decrease, as R increases, even though R is not connected in the exciter circuit. Now refer to Figure 26:

In explanation; as V_1 increases, only the charged droplets with the smaller mobility reach the ground screen 2. The charged droplets 3 with the greater mobility concentrate in a cloud at 4, and set up a repelling space charge field 5 which decreases the current I_2 to the exciter ring 6.

This suggests increasing the voltage V_2 and increasing the resistance R to increase I_1^2 R and decrease $V_2 I_2$; because I_2 will further decrease. This must be further investigated.

7. CONCLUSIONS

1. The hydraulic and electrical characteristics of Charging Method 5.1, an induction charged water jet, were obtained.

2. The hydraulic efficiency of various lengths of orifice 50 μm in diameter were determined. The efficiency increased to 67-70% for the shortest length 25 μm, which was greater than the conventional "book" value of 62% usually used.

3. The hydraulic efficiencies of various orifices 15, 25, 35, 50, and 100 μm diameter, all 25 μm long, were also obtained. For diameters smaller than 25 μm, the efficiency was nearly zero, and smaller orifices could not be used. The efficiency rapidly increased to the maximum at 50 μm diameter. These characteristics were ascribed to the "electroviscosity effect".

4. The efficiency also increased with pressure asymptotically to the maximum efficiency.

5. The electrical characteristics involved measuring the variables, input exciter voltage and current; and the output voltage and current, and computing input and output electric powers.

6. Important calculated variables were φ the charge density on the water in coulombs/m^3 and F_m, a Figure of Merit in μA/watt. It is shown that φ = 10 and F_m = 100 are values suitable for a practical generator with an output of 100,000 volts or more, and at a water pressure of 20 psig or less. In such case, the ratio of output power to input power (hydraulic + electric) will be at least 10; and the overall efficiency will be 90% or more. Only the 25 μm and 35 μm diameter orifices 25 μm long, met these criteria. The 35 μm diameter orifice is preferred because of greater hydraulic efficiency. A multi-orifice array will be required for a practical generator

as described herein.

7. The breakeven points where the electric power output and hydraulic power input are equal were determined. The 35 μm orifice (25 μm long) produces 10 times the power of the 25 μm orifice (25 μm long) and so the 35 μm diameter orifice (25 μm long) was chosen as the optimum.

8. An anomalous second breakeven point appears to be projected for a 50 μm orifice 25 μm long at about 100 psig, at a power increase of about 300 times relative to the first breakeven point. This remains to be investigated. If confirmed, it would decrease the number of orifices required by a factor of about 300, to 120/m^2.

9. Late in the contract, theoretical considerations led to the investigation of tubular exciter electrodes resulting in an order of magnitude increase in output current and 2 orders of magnitude in output power. The value of φ greatly increased. We have some preliminary results, but further work is needed to more fully characterize and optimize these results.

10. It was determined theoretically that a multiorifice array having n_a orifices would have very favorable scaling characteristics since the output electric power scales with n_a^2 while the hydraulic power input and electric power input scale as n_a, until the required voltage is reached. A scaleup for the 1-100 megawatt output range was made. For example, the output electric power at 20 psig is 45 MW and the total input power is 1.23 MW.

11. The water flow rate is large, but can be managed. For example, with the output voltage $V_1 = 10^6$ volts, and $\varphi = 10$ c/m^3 the water flow rate is about 38 gph/m^2. At smaller voltages, the flow rate is proportionally greater. However, a means of

water recuperation, and pressure regeneration has been invented and is disclosed herein intended to obviate this problem. Through the use of this invention in one or more embodiments, the water power is essentially free.

12. In a circular orifice in a thin sheet the net generated electric power exceeds the input power, and multiple sources should achieve greater voltage and current output.

13. With a suitable optimum charged aerosol, the transduction of wind power to electric power occurs efficiently (70 to 97%) at a wide range of ambient temperatures (20 to 40°C) and relative humidities (25 to 97%), at wind velocities of 2.5 to 16 m/s. This shows that a charged aerosol wind/electric power generator can be expected to operate over a wide range of atmospheric conditions.

8. SUMMARY

Summarizing the important results in this contract:

1. With an orifice of 50 μm diameter or greater, 67-70% hydraulic efficiency is obtained at a pressure of 7×10^4 n/m^2 (10 psig), or more. With an orifice diameter of 35 μm the hydraulic efficiency is 22% at 10 psig and 63% at 80 psig. The value of φ in c/m^3 increases as the orifice diameter decreases, as shown in Figure 22.

2. The smallest orifice combining an adequate hydraulic efficiency with $\varphi \approx 10$ is 35 μm diameter and 25 μm long.

3. The current per orifice of 0.1 μA for a plate orifice 35 μm diameter and 25 μm long. A structure is proposed to provide the required current per unit area (see Figures 28 and 29).

4. The design voltage across the load is 1.12×10^6 volts. For a value of $\varphi \approx 10$,

water pressure required is 1.4×10^4 n/m^2 (20 psig).

5. Given these values for the variables, the ratio of output electric power to all input power is about 10.

6. A scaleup to a 45 MW WPG is given.

7. A water recuperation and pressure recovery means has been invented in which water is conserved and the water power is freely provided by the wind and the gravitational field.

9. FURTHER WORK

Further work should be pursued simultaneously on basic studies, and engineering design each at a level of at least $150,000 per year.

9.1 Basic Studies

Continued study of the electrical/hydraulic characteristics of the single orifice

9.1.1 in the range 35 - 50 μm diameter and lengths 25 - 100 μm;

9.1.2 with tubular exciter

9.1.3 at increased pressures 70-200 psig

9.1.4 multiorifice arrays of various diameters, spacings and number of orifices

9.2 Engineering

9.2.1 Construction and test of a 32x32 = 1024 array multiorifice emitter to emit a charged aerosol with an electric current of about 0.1 milliampere at a water pressure of 20 psig.

9.2.2 Construction and test of a 6x6 superarray of arrays 9.2.1 in a 1 m^2 module.

9.2.3 Construction and test of a full scale Wind Power Generator to generate 10 kW in a 10 m/s wind to comprise a screen of 5x5 = 25 modules covering a square 5 m x 5 m, in the atmosphere.

10. LIST OF FIGURES

1. Experimental setup of water jet with induction electric charging.

2. Tubular Orifice design.

3. Plate Orifice design.

4. Appearance of a water jet during charged aerosol formation.

5. Electric Induction charging of water jet along the axis of a tublar exciter showing a cross sectional side view of jet.

6. Electric Induction charging of a water jet along the axis of a tublar exciter showing front sectional view.

7. Percent Hydraulic Efficiency vs. Pressure for a constant orifice length (25 μm) for various Orifice Diameters (25, 35, 50, 100 μm).

8. Percent Hydraulic Efficiency vs. Orifice Diameter in μm for constant Orifice Length (25 μm) for various Water Pressures P_r in psig.

9. Percent Hydraulic Efficiency vs. Orifice Length in μm for constant Orifice Diameter (50 μm) at various Water Pressures P_r in psig.

10. Velocity of water jet vs. Water Pressure P_r in psig for various Orifice Diameters in μm at constant Orifice Length (25 μm).

11. Input and Output Power in Watts vs. Water Pressure in psig for a tubular nozzle 2000 μm long and 76 μm diameter.

12. Input and Output Power vs. Water Pressure for a tubular nozzle 2000 μm long and 50 μm diameter.

13. Input and Output Power vs. Water Pressure for a tubular nozzle 1000 μm long and 50 μm diameter.

14. Input and Output Power in Watts vs. Water Pressure in psig for a 74 x 100 μm diameter plate Orifice 50 μm long.

15. Input and Output Power vs. Water Pressure for a plate Orifice 50 μm diameter and 25 μm long.

16. Input and Output Power vs. Water Pressure for a plate Orifice 35 μm diameter and 25 μm long.

10. LIST OF FIGURES (Continued)

17. Input and Output Power vs. Water Pressure for a plate Orifice 25 μm diameter and 25 μm long.

18. Projected output and input power using a 10 multi-orifice plate array having Orifices 35 μm diameter and 25 μm long.

19. Output Current in μA and Output Voltage in kV vs. Exciter Voltage in kV at various water pressures in psig, for plate orifice 25 μm dia. and 25 μm long.

20. Output and Input Currents vs. Exciter Voltage at constant Pressure P_r for a plate orifice 50 μm diameter and 25 μm long.

21. Output and Input Currents $I_1 = I_2$ μA, Output and Input Voltages V_1, V_2 kv vs. Water Pressure P_r psig plate orifice 50 μm diameter and 25 μm long.

22. Relationship between the Electric Charge Density φ on the water droplet, and Water Pressure P_r (psig) for various plate orifice diameters; 25, 35, and 50 μm and constant length 25 μm.

23. Figure of Merit F_m (μA/Watt) vs Water Pressure P_r (psig) for plate orifices having various diameters; 25, 35, and 50 μm, for constant length 25 μm.

24. Plot of theoretical equation (61) showing Electric Charge Density on Water φ vs. Orifice diameter d_j in μm.

25. Input and Output Currents and Input and Output Voltages vs. Load Resistance (ohms) for the following conditions: d_j = 50 μm, P_r = 50 psig constant, V_2 = 10 kV constant, Exciter ring 60 mm diameter, constant flow rate $Q = 4.4 \times 10^{-8}$ m^3/s and constant wind velocity U_w = 7.5 m/s.

26. A diagram of a Water Jet with Induction Electric Charging with self-limiting Exciter Current due to increasing Space Charge Field.

27. Wind/Electric Power Generator with Water Recuperation & Pressure Regeneratic

28. Design for a multi-orifice plate array 32 x 32 or 1,024 35 μm diameter Orifices 25 μm long. Magnified Views: Figure 28.1: Plan View Scale 10:1; Figure 28.2: Cross section Scale 10:1; Figure 28.3: Plan View Scale 320:1; Figure 28.4: Cross sectional side view Scale 320:1.

29. Design for a 1 m^2 Module for use in a multi-module Wind/Electric Power range in the kilowatt or megawatt category.

10. LIST OF FIGURES (Continued)

30. For a Tubular Exciter, Output Current vs. Exciter-Emitter voltage.

31. For a Tubular Exciter, Output Current vs. Length of the Exciter Tube.

32. Output Power and % Electric Efficiency vs. Air Temperature °C for various Relative Humidities %.

33. % Efficiency, electric vs. Wind Velocity

34. Projected Multimegawatt Output and Input Power having Superarrays of Multi-orifices, each 35 μm diameter and 25 μm long, scaled to 10^5 m^2.

11. REFERENCES

1. U. S. Patent 2,638,555, issued May 12, 1953, entitled "Heat-Electrical Power Conversion Through the Medium of a Charged Aerosol".

2. U. S. Patent 3,518,461, issued June 20, 1970, entitled "Charged Aerosol Power Conversion Device and Method".
   2.1 Column 16, lines 1-53 and Figure 10.

3. "Optimum Charged Aerosols for Power Conversion", J. Appl. Phys., Vol. 43, No. 1, January 1972, page 227, Case IV .

4. Letter dated December 30, 1971 to William M. Magruder, Special Consultand to the President, The White House, Washington, DC 20500.

5. Letter from Dr. Edward E. David, Science Adviser to the President, The White House, Washington, DC, dated February 25, 1972.

6. Proposal 73-1007 dated October 25, 1973, entitled "Wind Power Charged Aerosol Generator" sent to the National Science Foundation.

7. Proposal/Grant AER 74-18650 for the period October 1, 1975 through June 30, 1976.
   7.1 Final Report dated September 1976, page 40, A-3.

8. Contract EG-77-C-01-4002 for the period January 10, 1976 through June 30, 1977; Contract EG-77-C-01-2774 for the period September 27, 1977 through September 26, 1978.

9. Contract XH-9-8128-1 for the period May 1, 1979 through April 30, 1980.

10. "Electrofluid Dynamic (EFD) Wind Driven Generator Research", by Minardi, J.E., and Lawson, M.O., presented at the Society of Engineering Sciences, Inc., November 14, 15, 16, 1977, Lehigh University.

11. "Conversion Eolienne Electrostatique", Ricateau, Pierre and Zettwoog, Pierre, reprinted from "La Meteorologie", September 1977 pp 123-130.

12. Letter to President Jimmy Carter dated July 9, 1979.

13. Letter to Dr. Deutch + Technical Reply Memorandum dated October 1, 1979.

14. Elton, G.A.H. "Electroviscosity I", The Flow of Liquids Between Surfaces in Close Proximity, Proc. Royal Soc., London A, 1948, 194, pp 259-74.

11. REFERENCES (Continued)

15. Jeans, J. H., Electricity and Magnetism, Cambridge at the University Press, Fifth Edition, 1927, pp 73-74 - Coaxial Cylinders - Capacity.

16. Medaugh, F.W., and Johnson, G.D., Civil Engr., July 1940, p 424.

17. Kent's Mechanical Engineers' Handbook "Power Volume" 12th Edition, New York, John Wiley & Sons, Inc., Section 1-22.

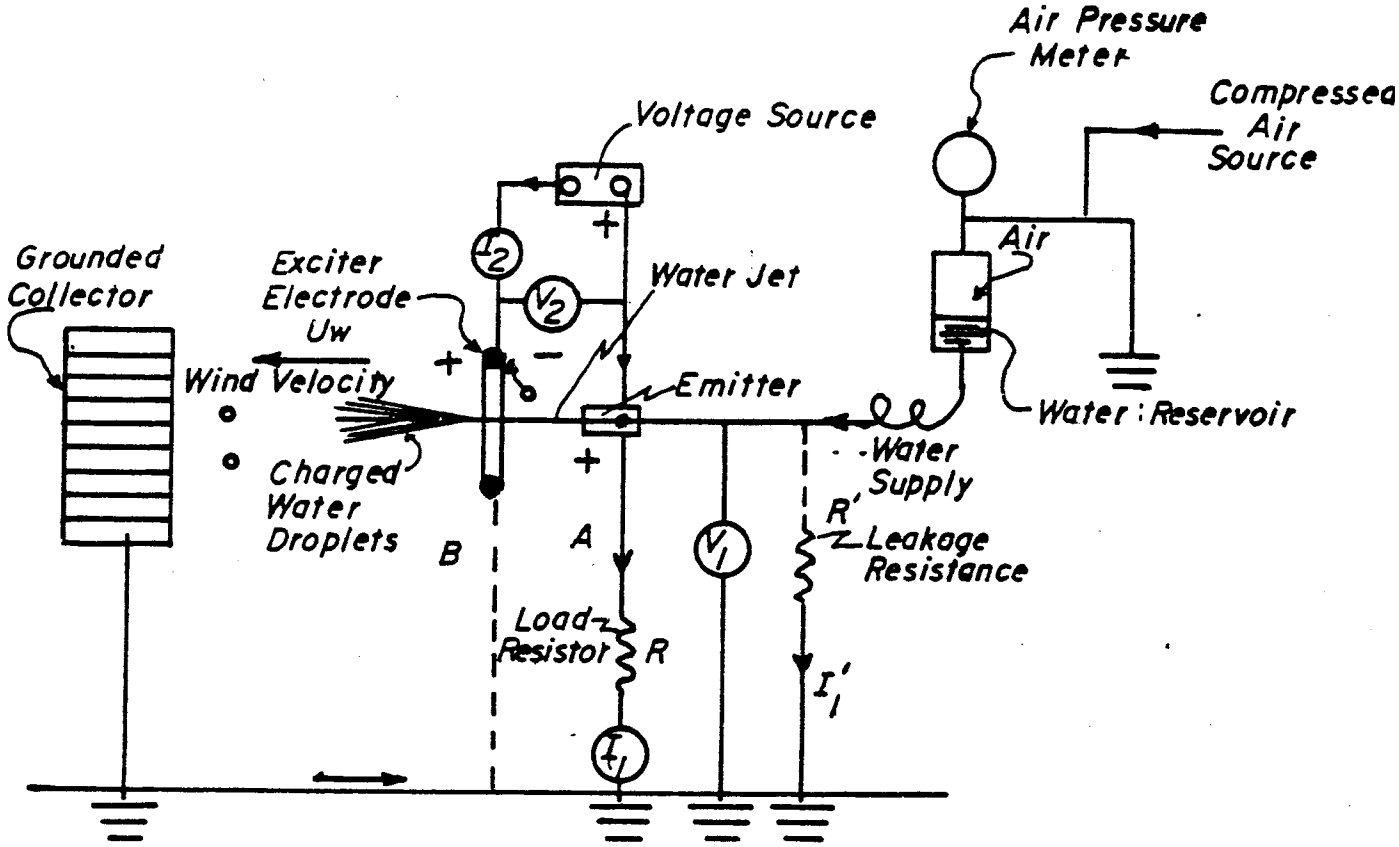

FIG. 1

EXPERIMENTAL SETUP OF WATER JET WITH INDUCTION ELECTRIC CHARGING

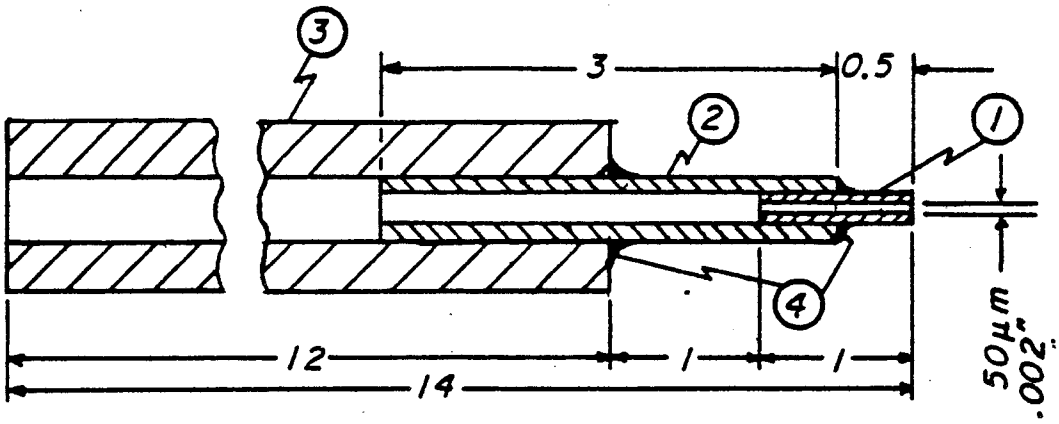

ITEM NO.	O.D.	I.D.	L.	MATERIAL
1	.005"	.002"	.040"	BRASS TUBING *
2	.016"	.006"	.120"	" "
3	.044"	.018"	.480"	" "
4	—	—	—	EPOXY or SOLDER

* Supplier
MOR-WEAR TOOLS INC
65 Saginaw Drive
Rochester N Y 14623

FIG. 2

50µm NOZZLE TUBE Scale: 20:1

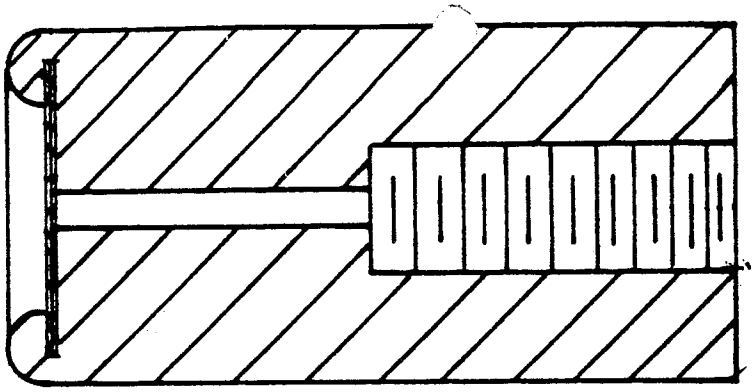

FIG. 3.1
Scale: 4:1

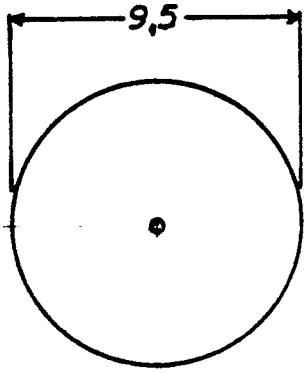

FIG. 3.2
DETAIL OF ORIFICE PLATE

FIG. 3.3
Scale: 4:1

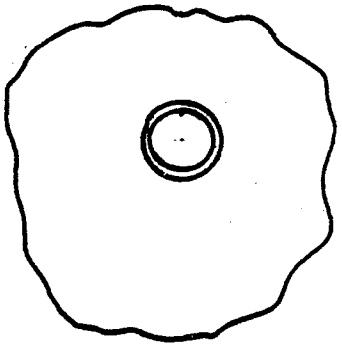

FIG. 3.4
MAGNIFIED VIEWS OF ORIFICE PLATE
Scale: 200:1

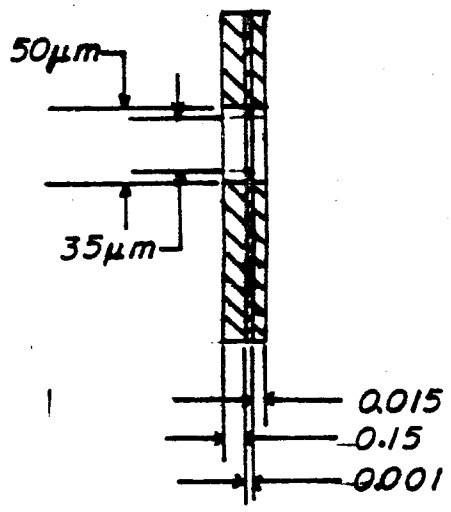

FIG. 3.5

FIG. 3

PLATE ORIFICE DESIGN

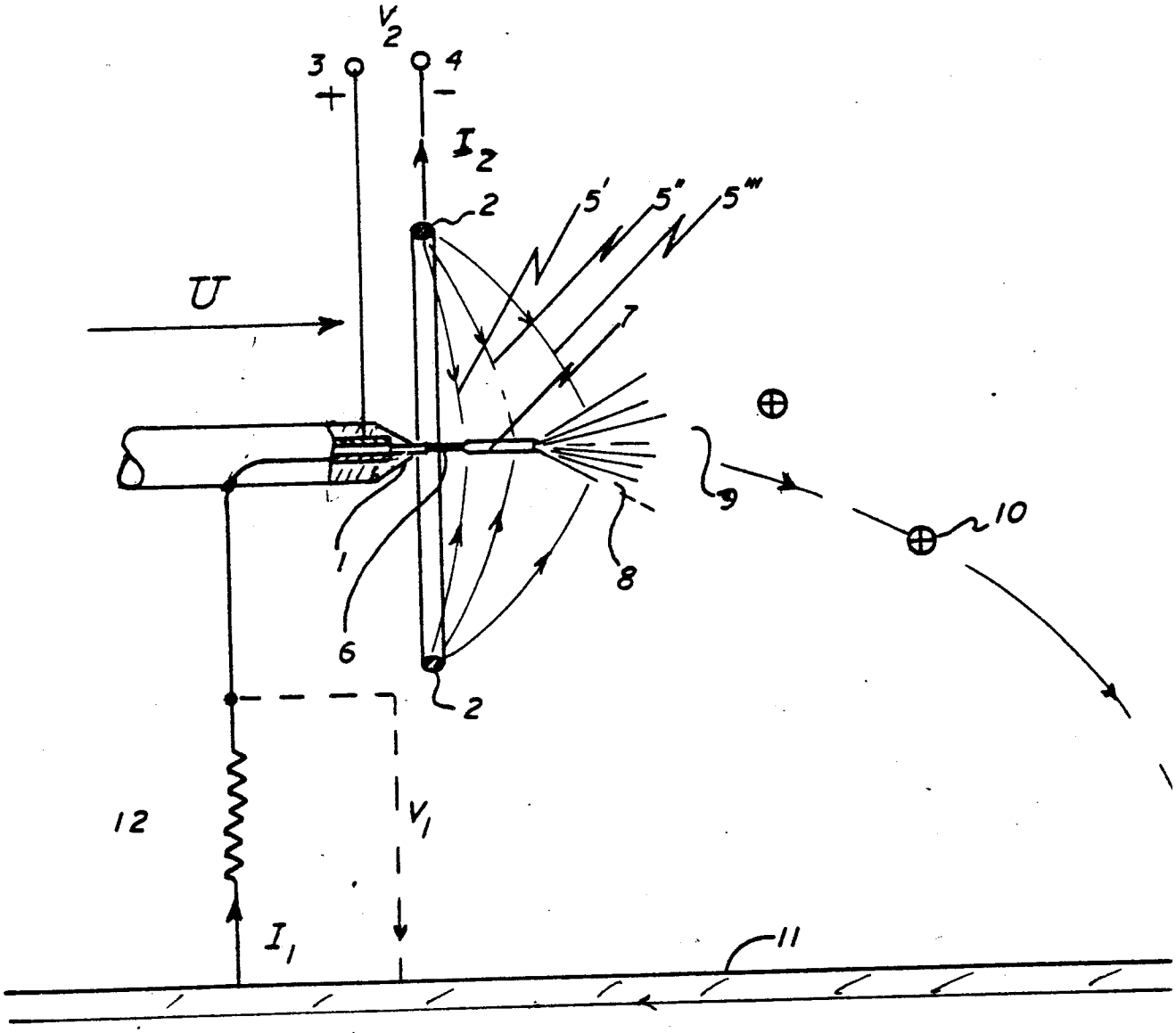

FIG. 4

APPEARANCE OF A WATER JET DURING CHARGED AEROSOL FORMATION

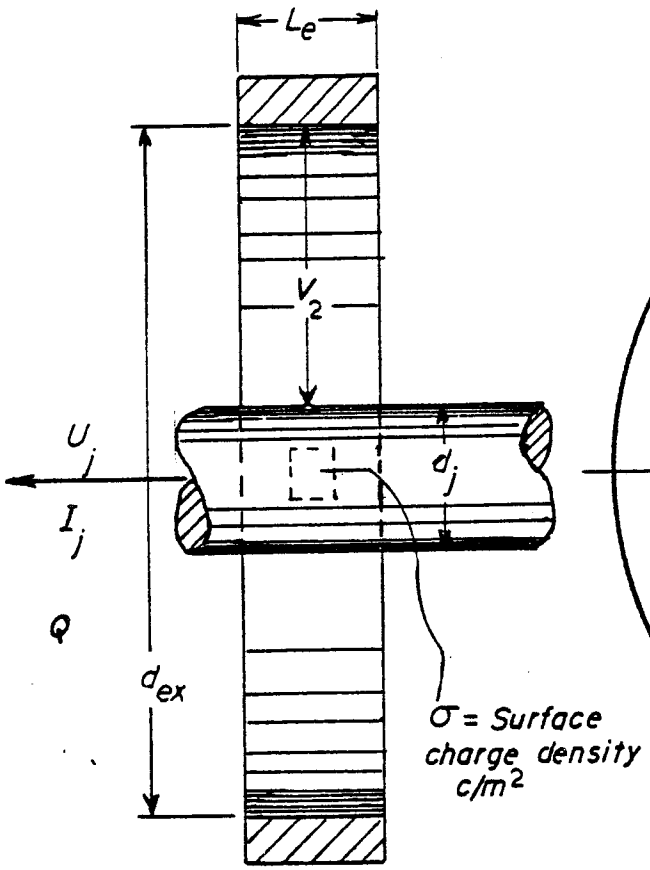

FIG. 5

CROSS SECTIONAL SIDE VIEW OF JET ALONG THE AXIS OF A TUBULAR EXCITER

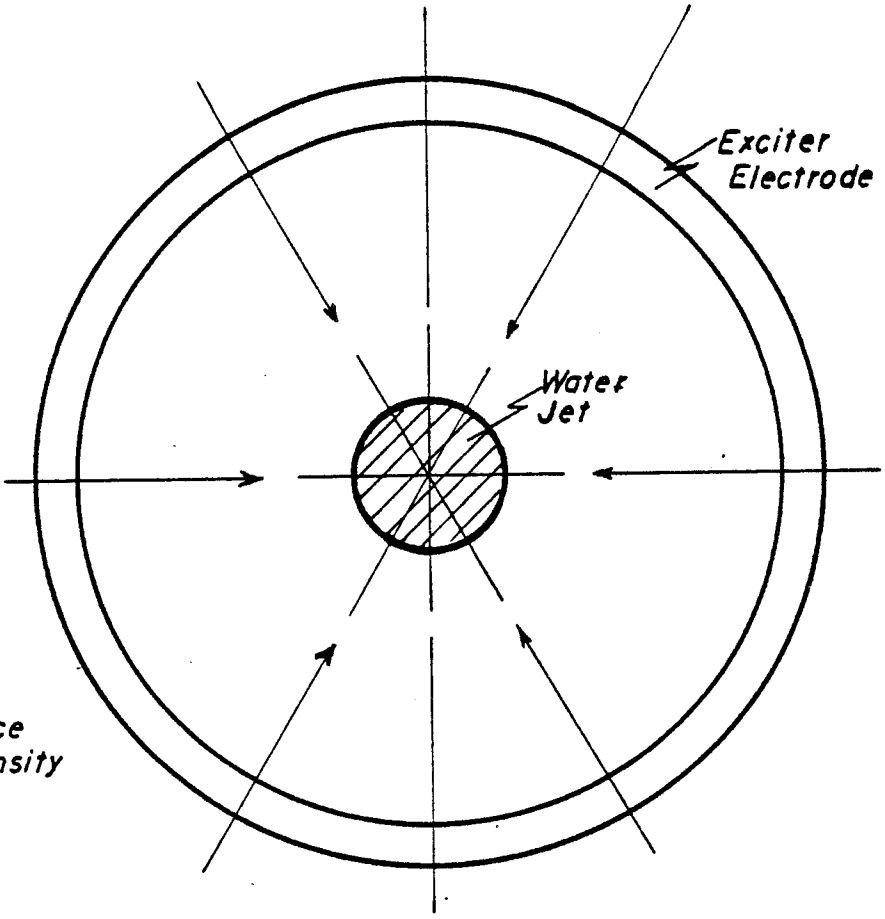

FIG. 6

FRONT SECTIONAL VIEW OF JET ALONG THE AXIS OF A TUBULAR EXCITER

ELECTRIC CHARGING OF WATER JET

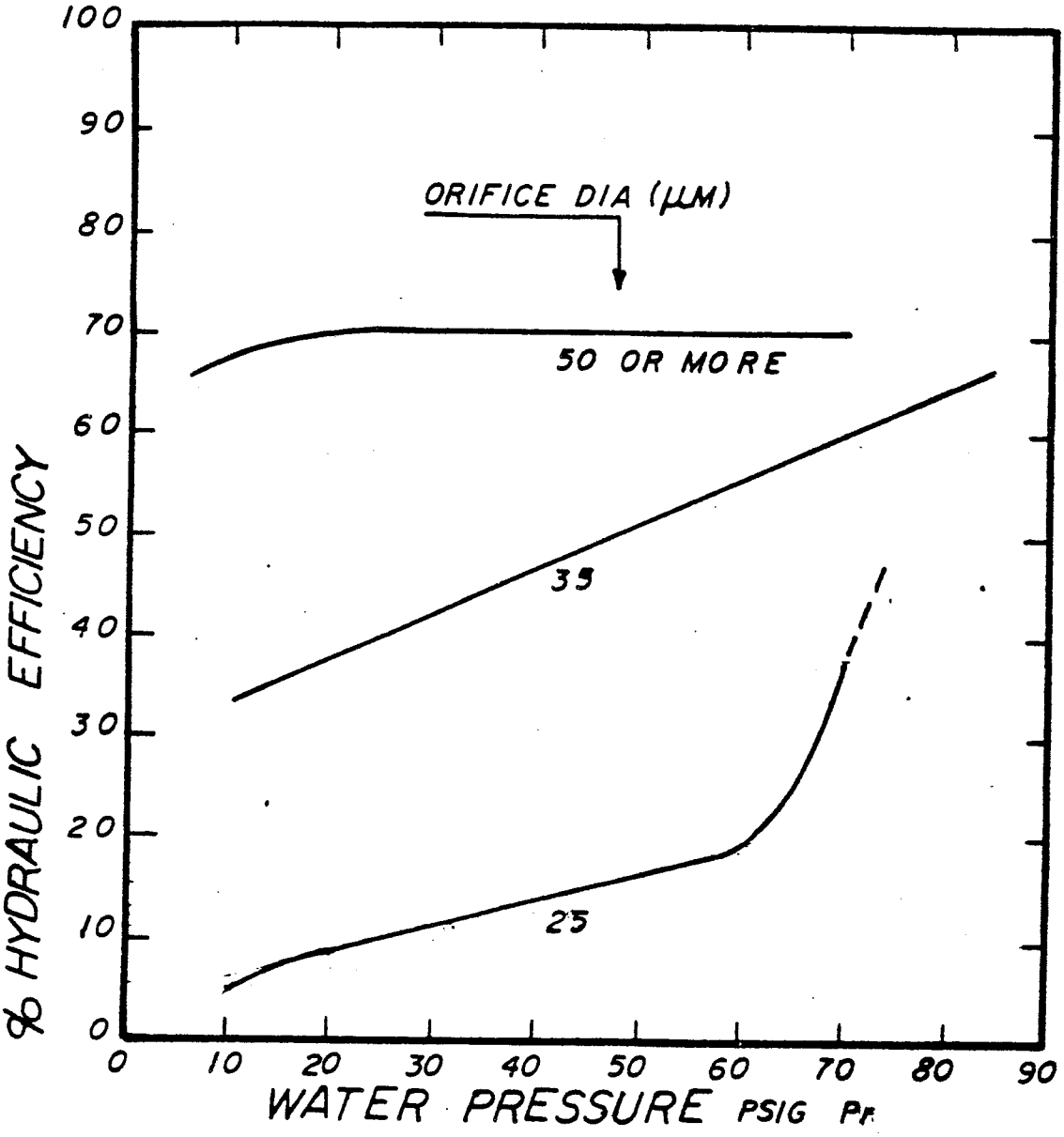

FIG. 7

PERGENT HYDRAULIC EFFICIENCY
vs
WATER PRESSURE P_r psig
FOR
VARIOUS ORIFICE DIAMETERS 25, 35, 50, 100 μm
FOR A
CONSTANT ORIFICE LENGRH 25 μm

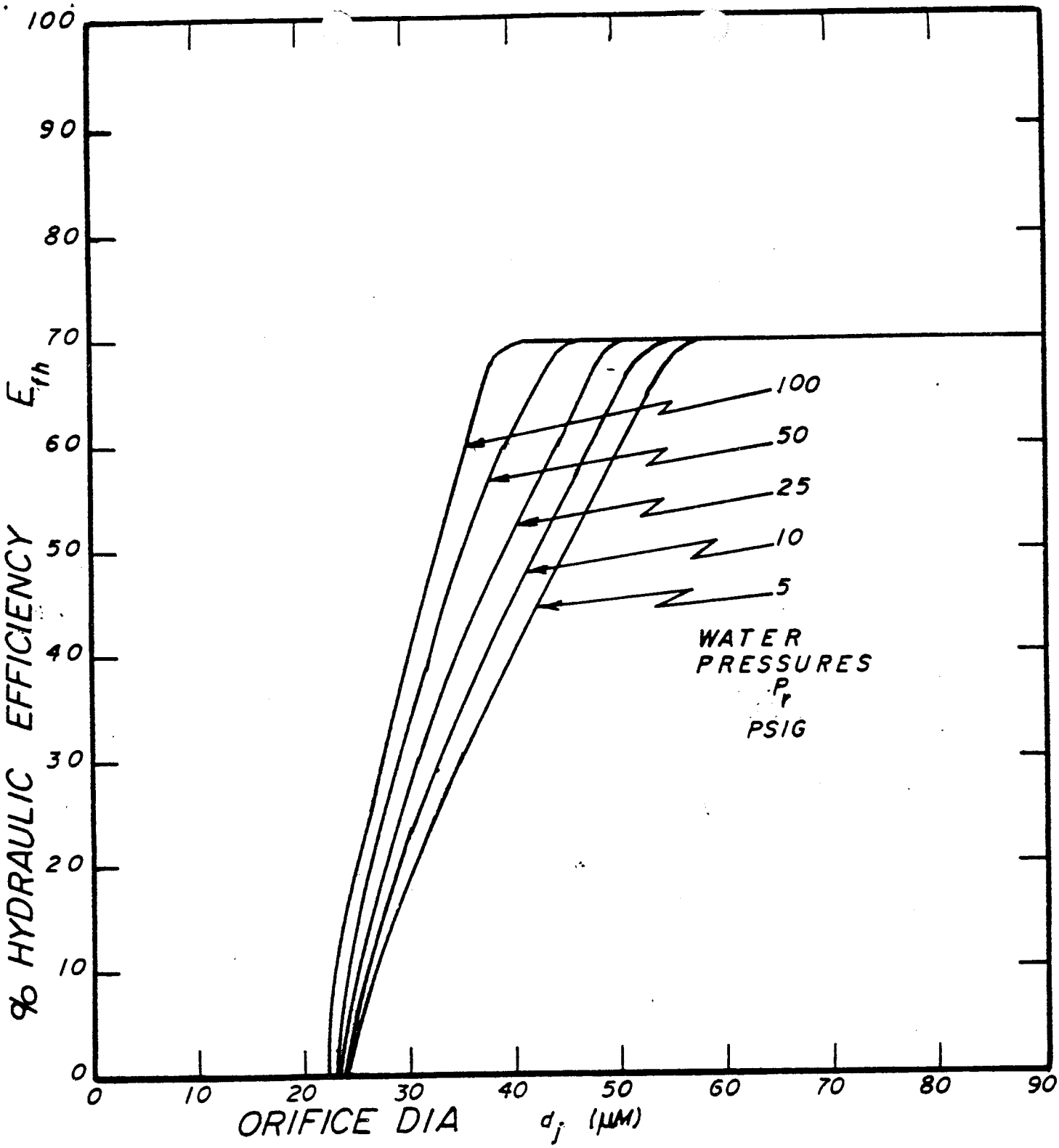

FIG. 8

PERCENT HYDRAULIC EFFICIENCY
vs
ORIFICE DIAMETER IN μm
FOR
CONSTANT LENGTH 25 μm
FOR
VARIOUS WATER PRESSURES P_r psig

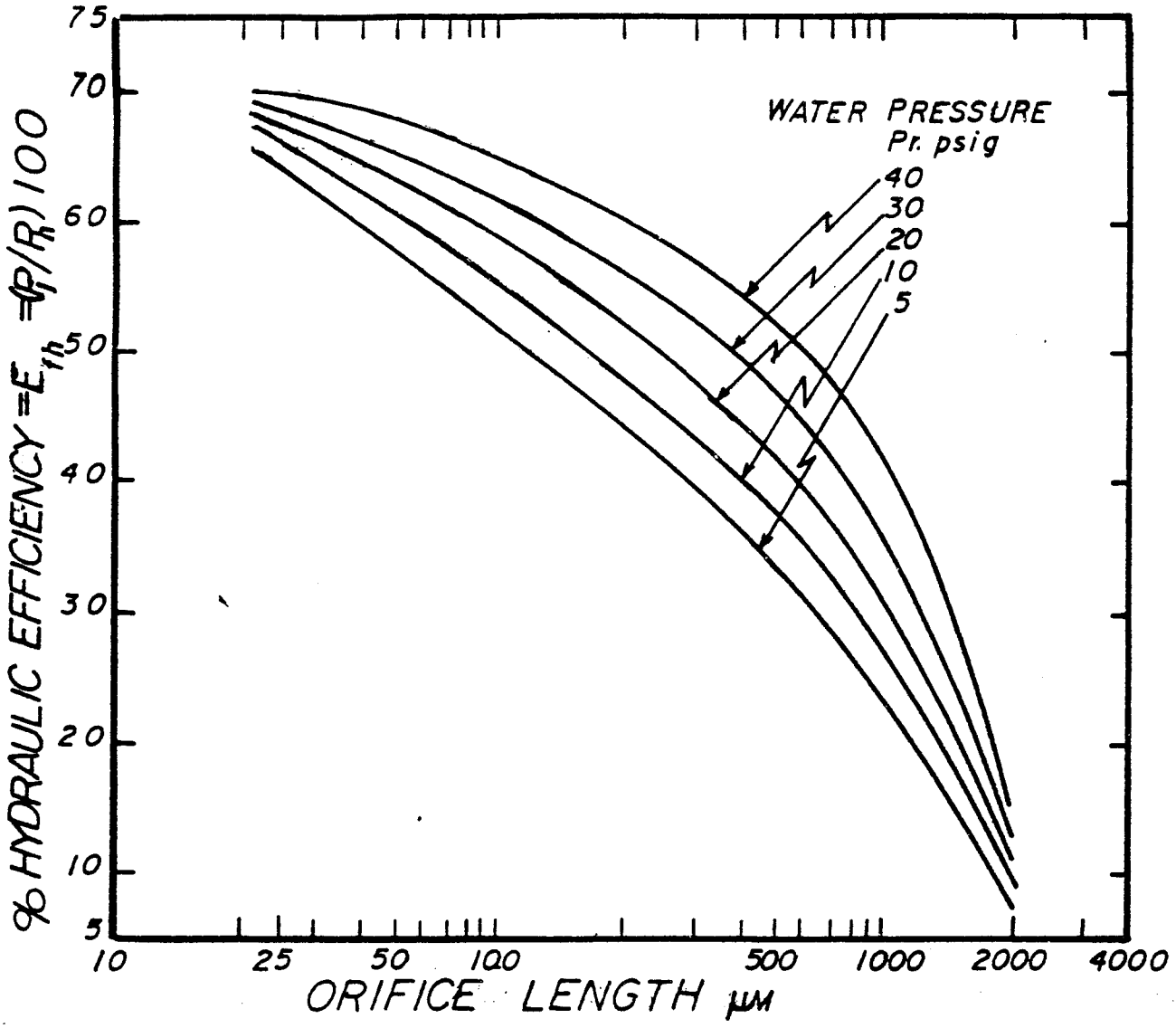

FIG. 9.

PERCENT HYDRAULIC EFFICIENCY
vs
ORIFICE LENGTH IN um
FOR
CONSTANT ORIFICE DIAMETER 50 μm
AT
VARIOUS WATER PRESSURES P_r psig

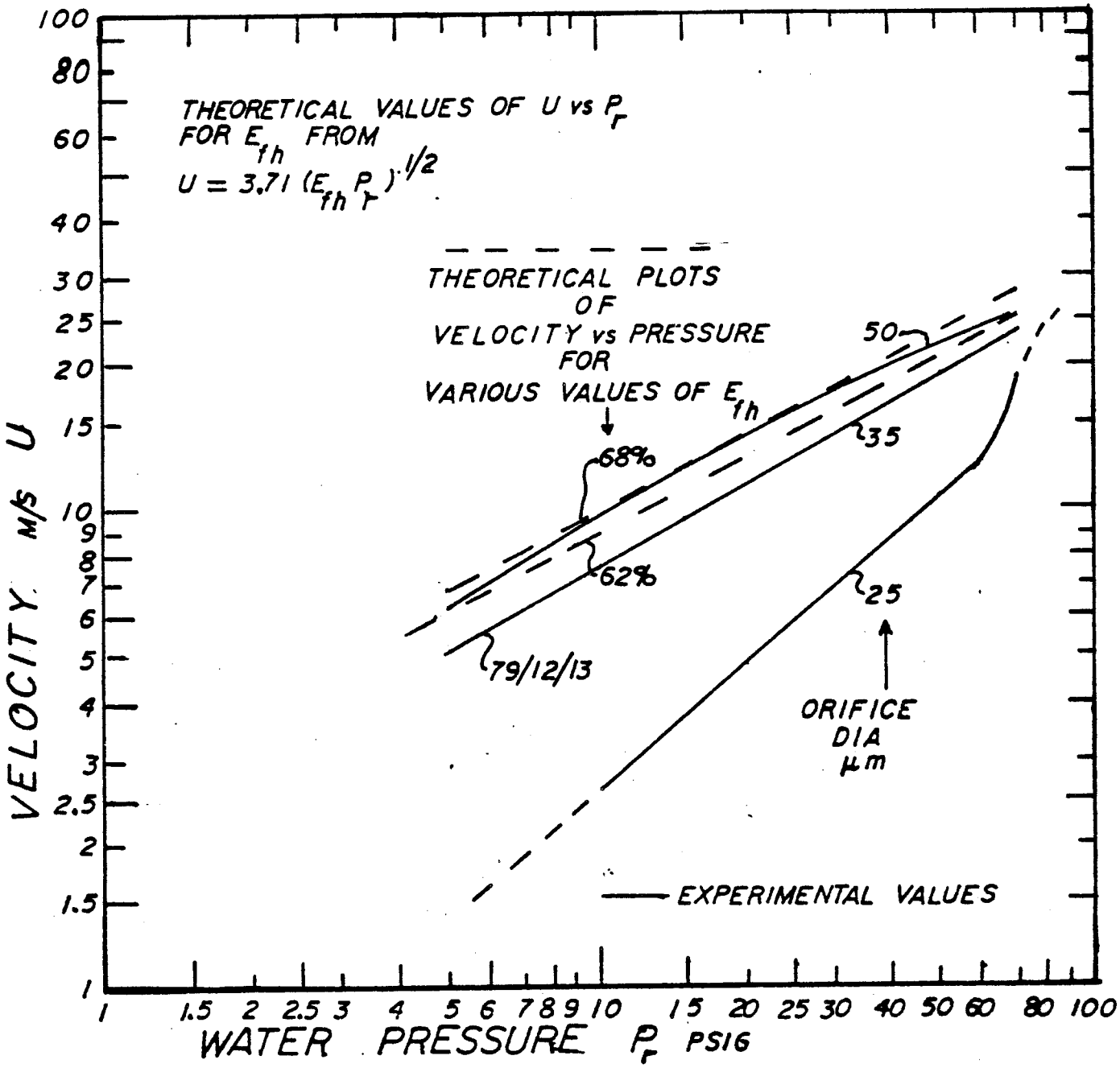

FIG. 10

JET VELOCITY m/s
vs
WATER PRESSURE P_r psig
FOR
VARIOUS PLATE ORIFICES 25, 35, 50 μm DIAMETER
OF
CONSTANT LENGTH 25 μm

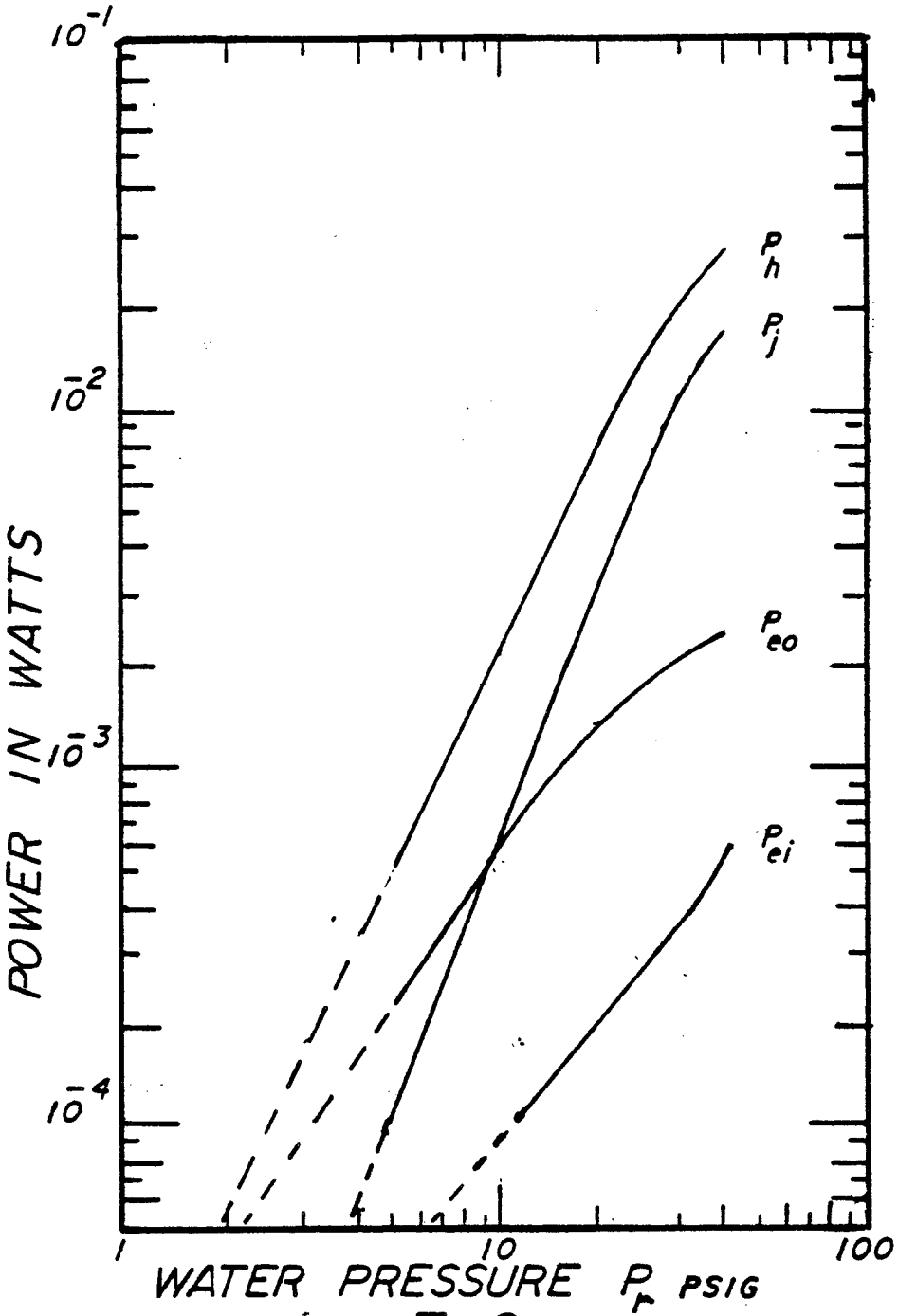

FIG. 11

INPUT AND OUTPUT POWER IN WATTS
vs
WATER PRESSURE P_r psig
FOR A
TUBE ORIFICE
76 μm DIAMETER
2000 μm LONG

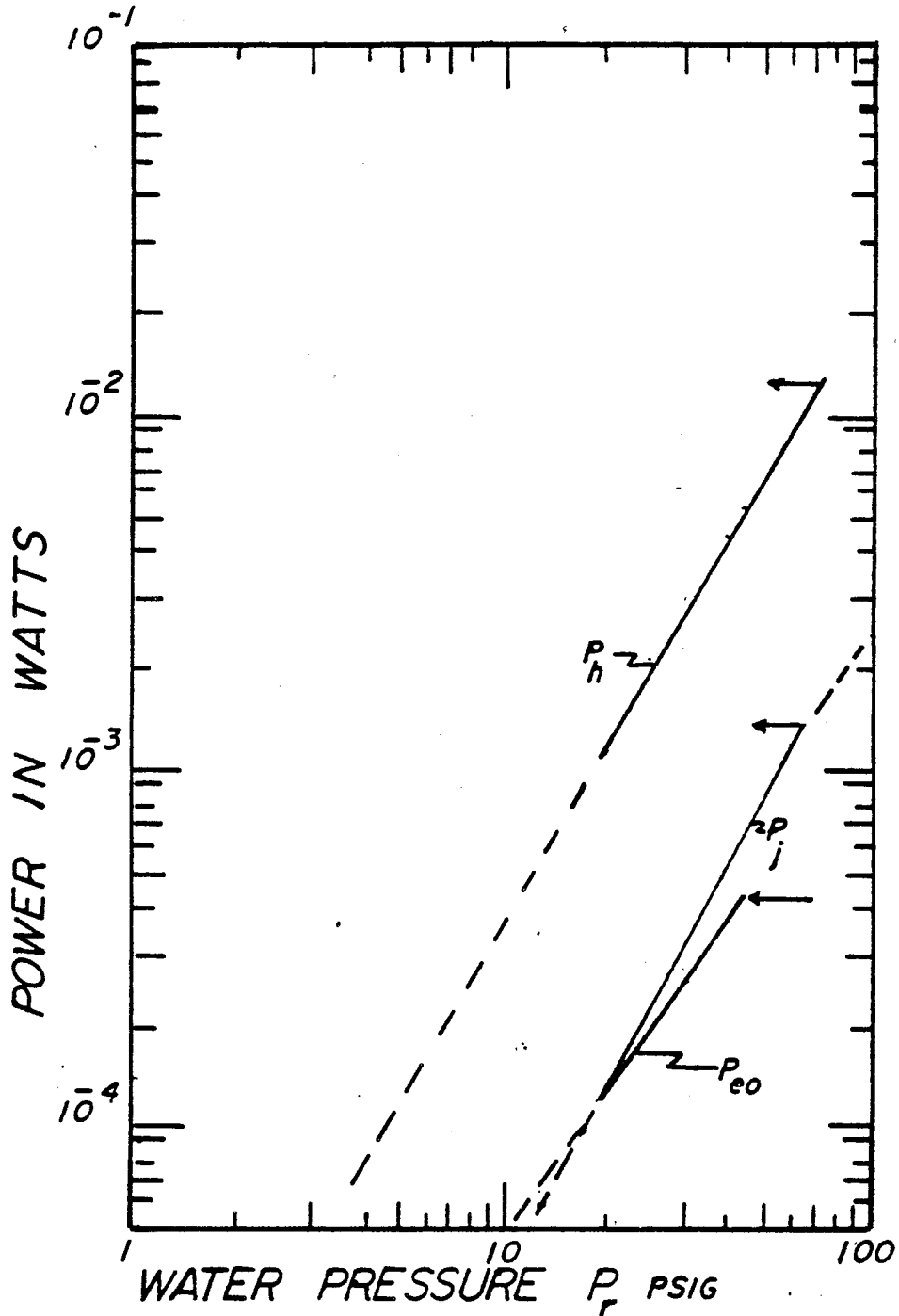

FIG. 12

INPUT AND OUTPUT POWER
vs
WATER PRESSURE P_r psig

FOR a
TUBE ORIFICE
50 μm DIAMETER
2000 μm LONG

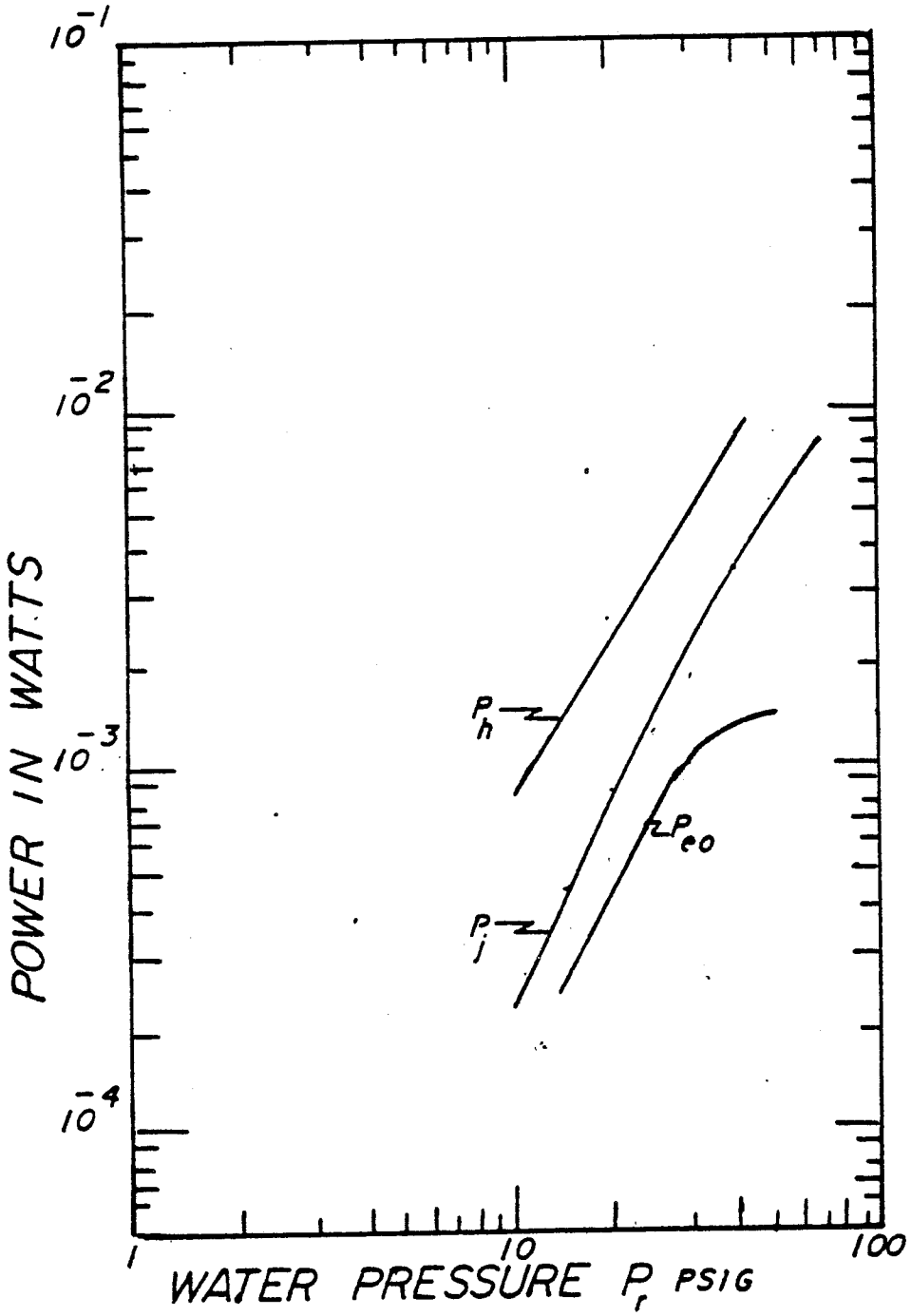

FIG. 13

HYDRAULIC POWER P_h, KINETIC POWER P_j, ELECTRIC POWER INPUT P_{ei}
and
ELECTRIC POWER OUTPUT P_{eo}, IN WATTS
vs
WATER PRESSURE P_r IN psig
at
ORIFICE DIA 50 μm
and
ORIFICE LENGTH 1000 μm

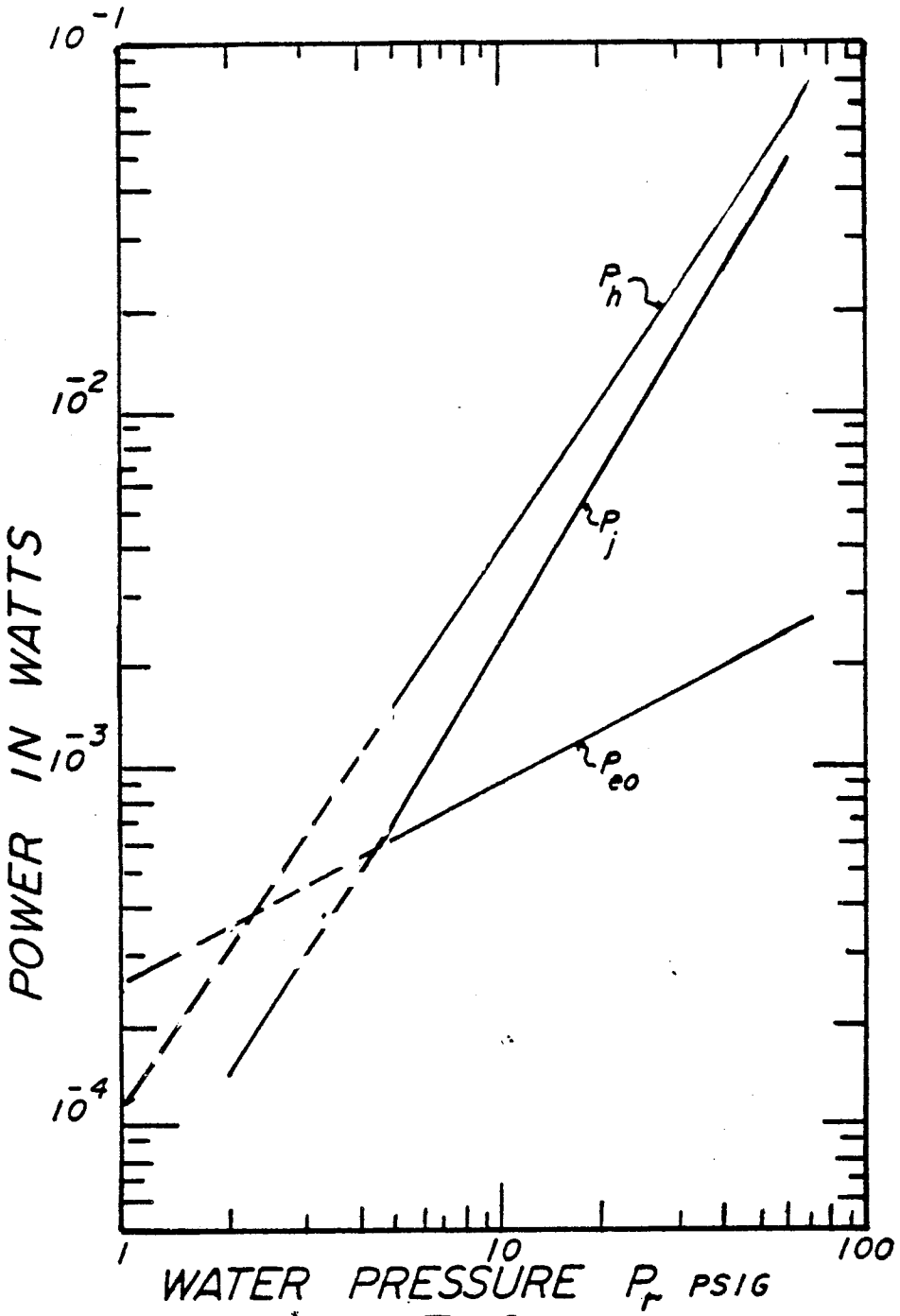

FIG. 14

INPUT AND OUTPUT POWER IN WATTS
vs
WATER PRESSURE IN PSIG
FOR
A PLATE ORIFICE
74 x 100 μm DIAMETER
50 μm LONG

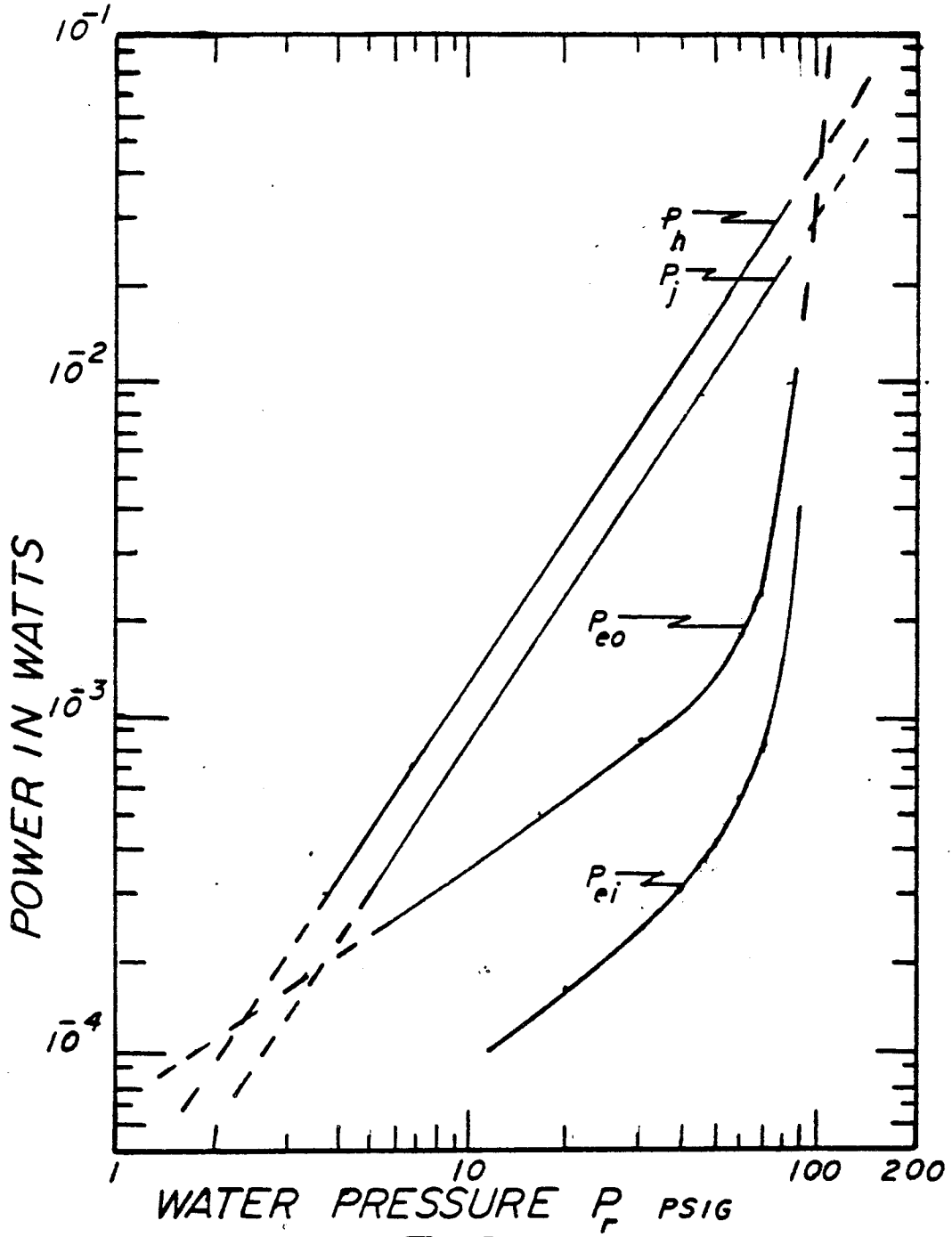

FIG. 15

INPUT AND OUTPUT POWER
vs
WATER PRESSURE
FOR
A PLATE ORIFICE
50 μm DIAMETER
25 μm LONG

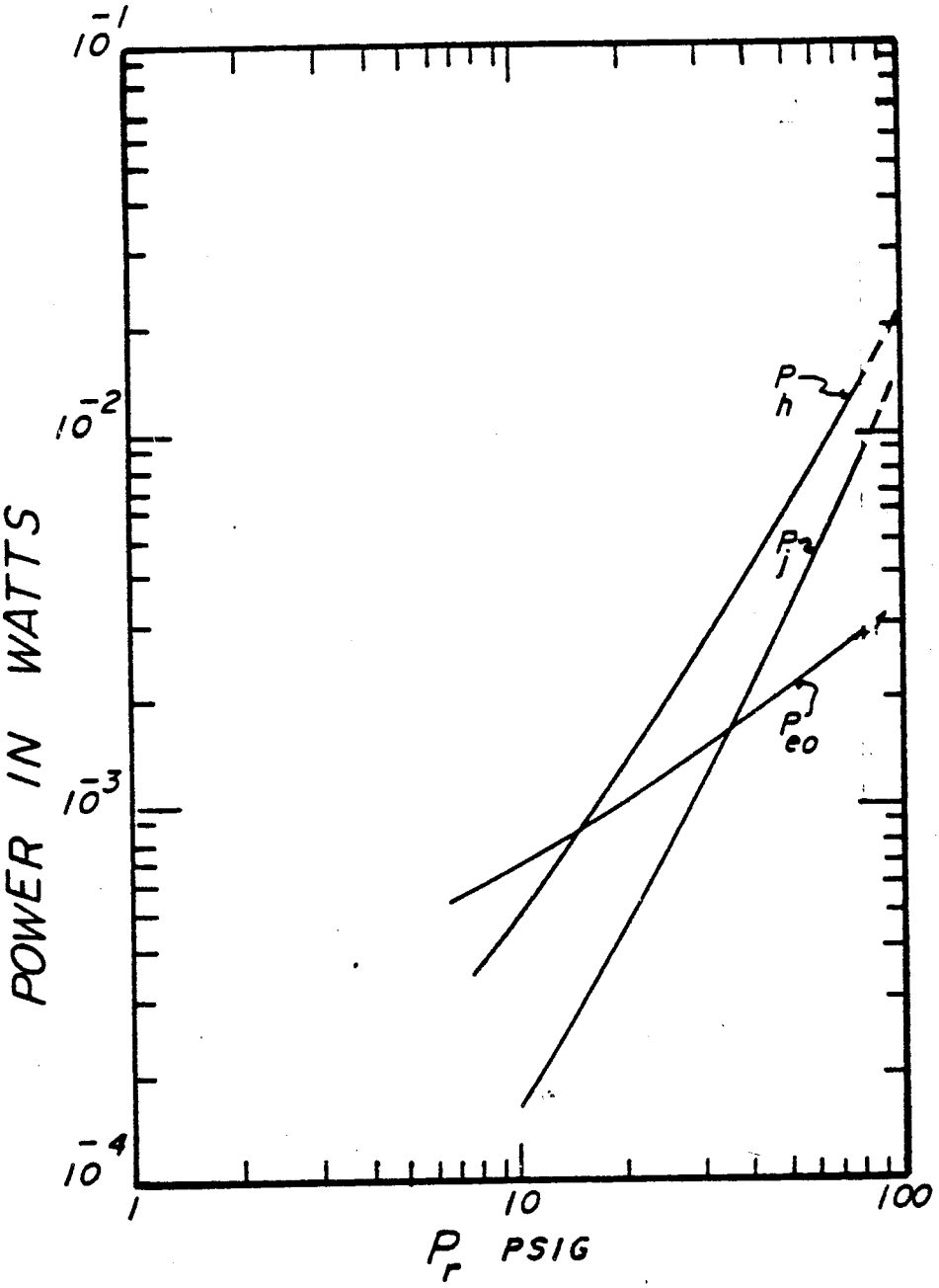

FIG. 16

INPUT AND OUTPUT POWER
vs
WATER PRESSURE
FOR
A PLATE ORIFICE
35 μm DIAMETER
25 μm LONG

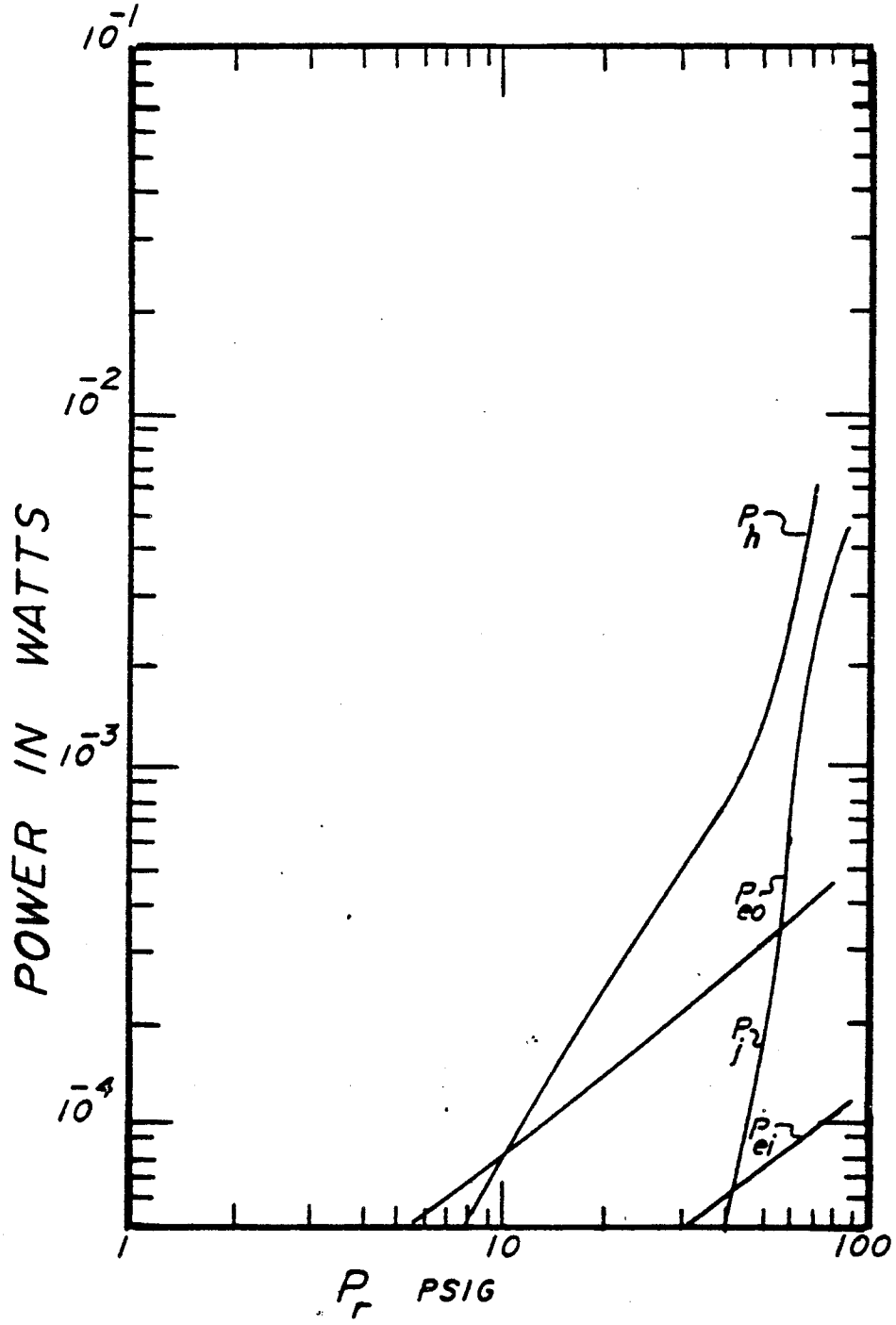

FIG. 17

INPUT AND OUTPUT POWER WATTS
vs
WATER PRESSURE P_r psig
FOR
A PLATE ORIFICE
25 μm DIAMETER
25 μm LONG

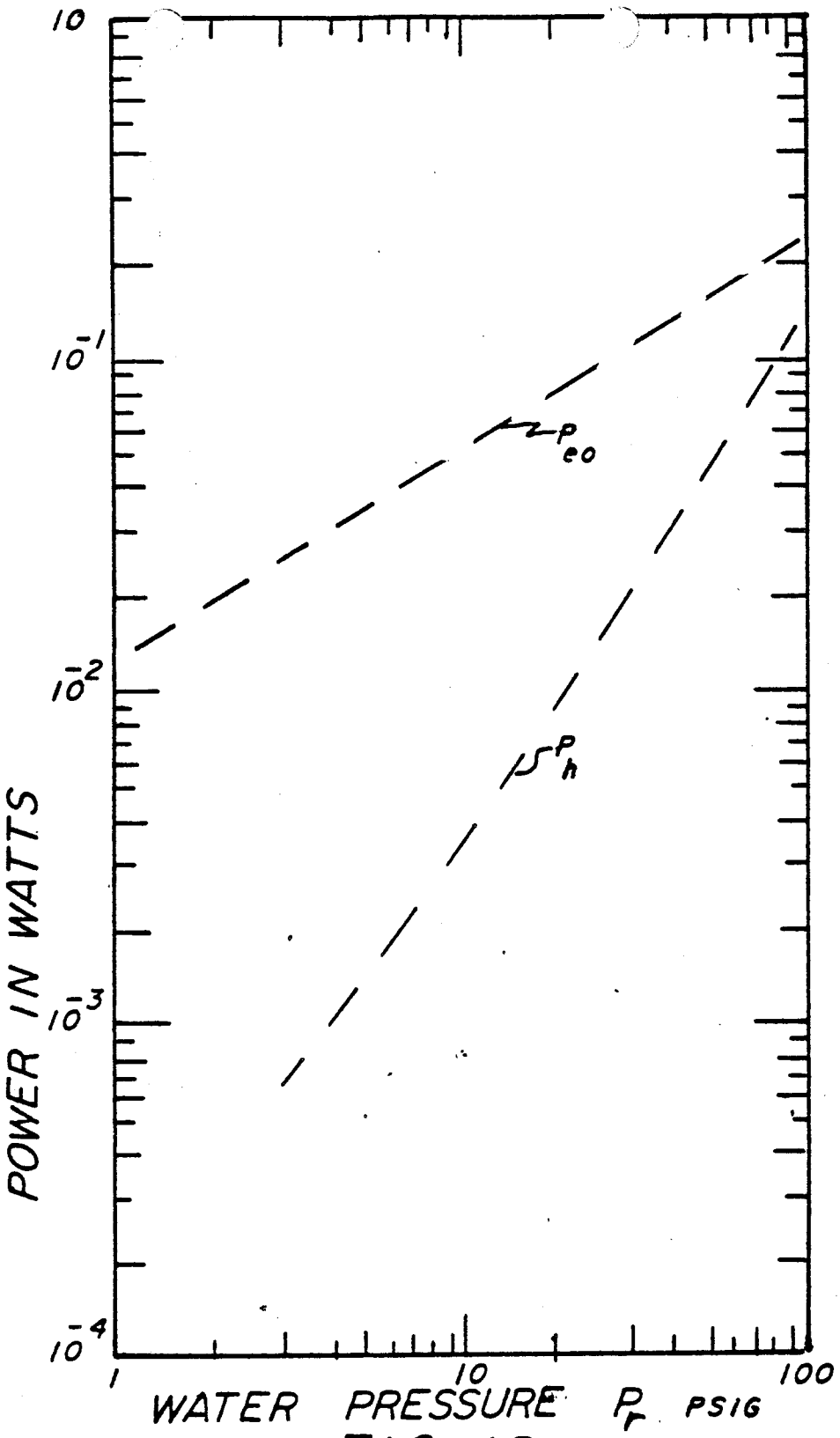

FIG. 18

PROJECTED ELECTRIC OUTPUT AND HYDRAULIC INPUT
POWER IN WATTS
FOR A
3 x 3 = 9 MULTI-ORIFICE PLATE ARRAY HAVING ORIFICES
35 μm DIAMETER
AND
25 μm LONG

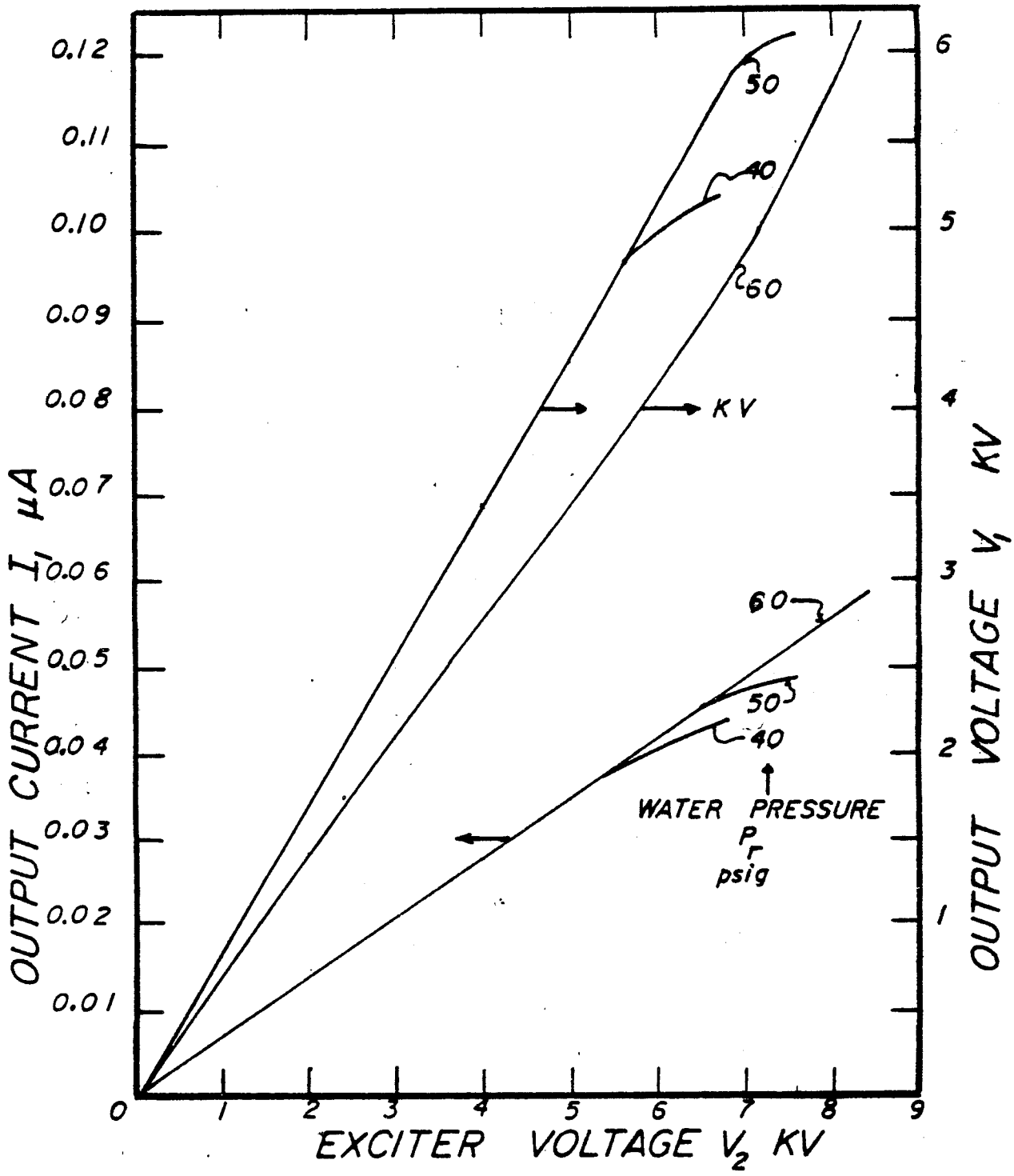

FIG. 19

OUTPUT CURRENT I_1 μA
AND
OUTPUT VOLTAGE V_1 kV
vs
EXCITER VOLTAGE V_2 kV
FOR
VARIOUS WATER PRESSURES P_r psig

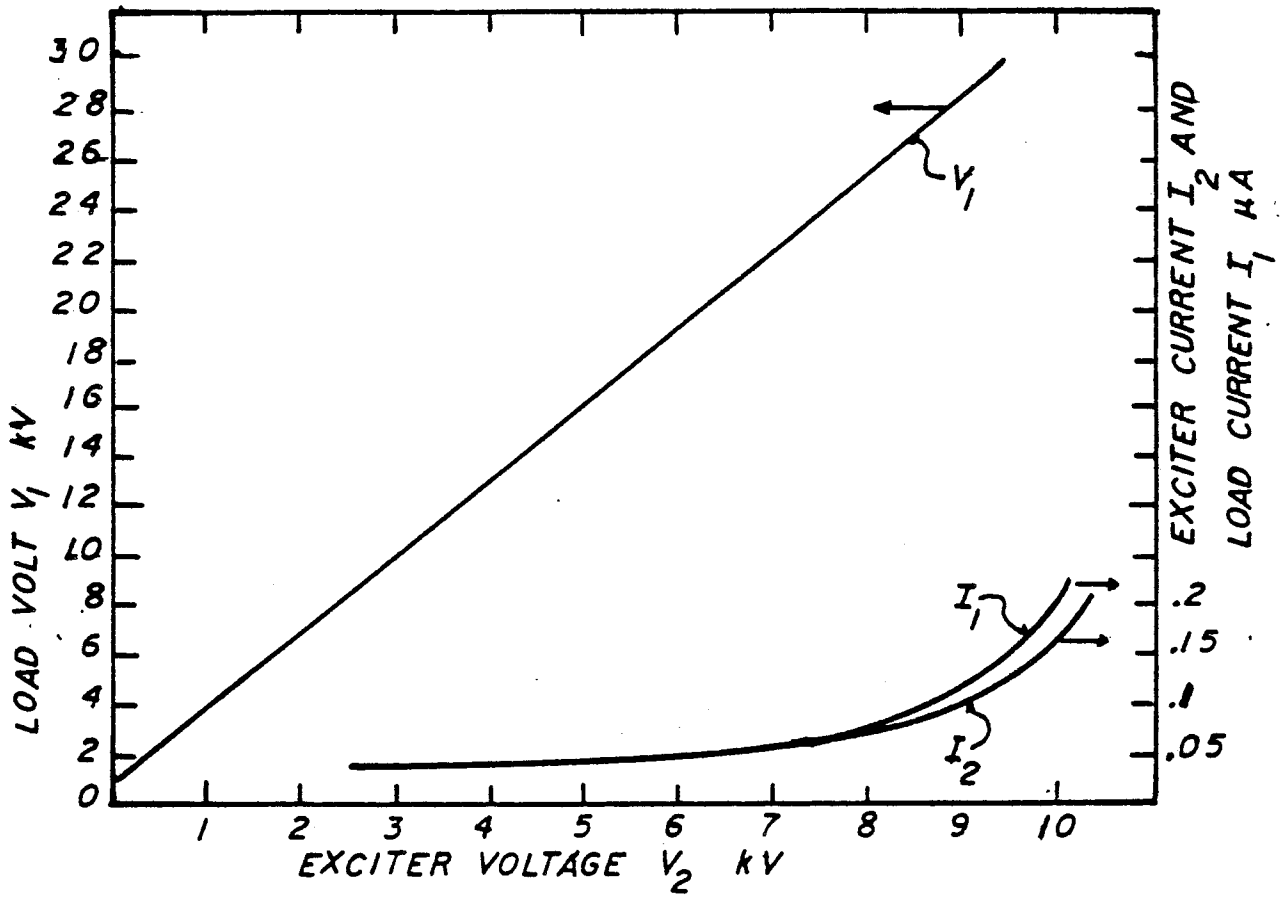

FIG. 20

EXCITER VOLTAGE V_2
vs
LOAD VOLTAGE V_1
AND
BOTH EXCITER CURRENT I_2
AND
LOAD CURRENT I_1
AT CONSTANT WATER PRESSURE P_r = 50 psig
FOR
OFIFICE DIAMETER 50 μm
AND
25 μm LONG

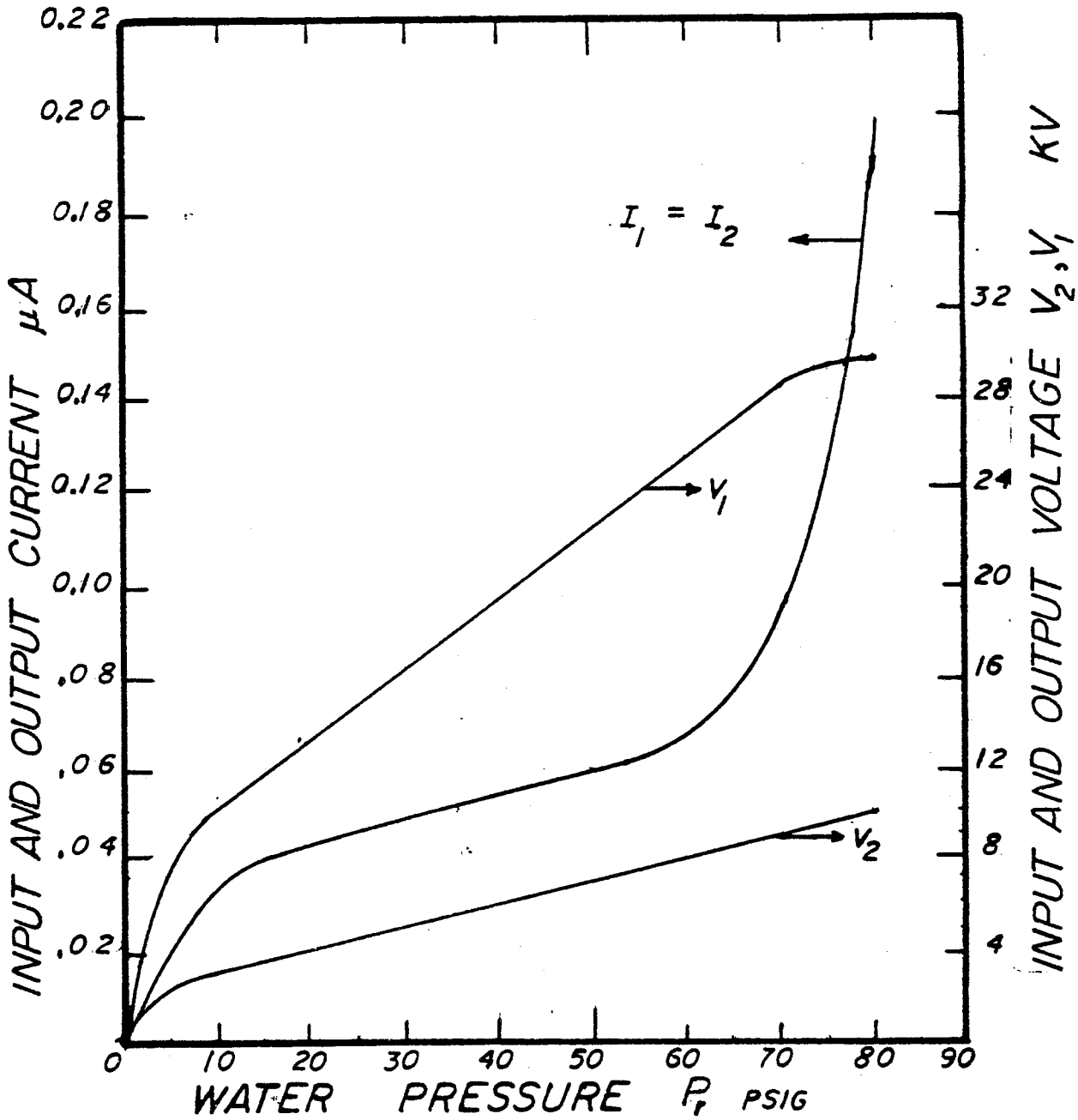

FIG. 21

OUTPUT CURRENT I_1
AND
INPUT CURRENT I_2 μA
AND
OUTPUT AND INPUT VOLTAGES V_1 and V_2 kV
vs
WATER PRESSURE P_r psig
IN WHICH $I_1 = I_2$
FOR
A PLATE ORIFICE 50 μm DIAMETER
AND
25 μm LONG

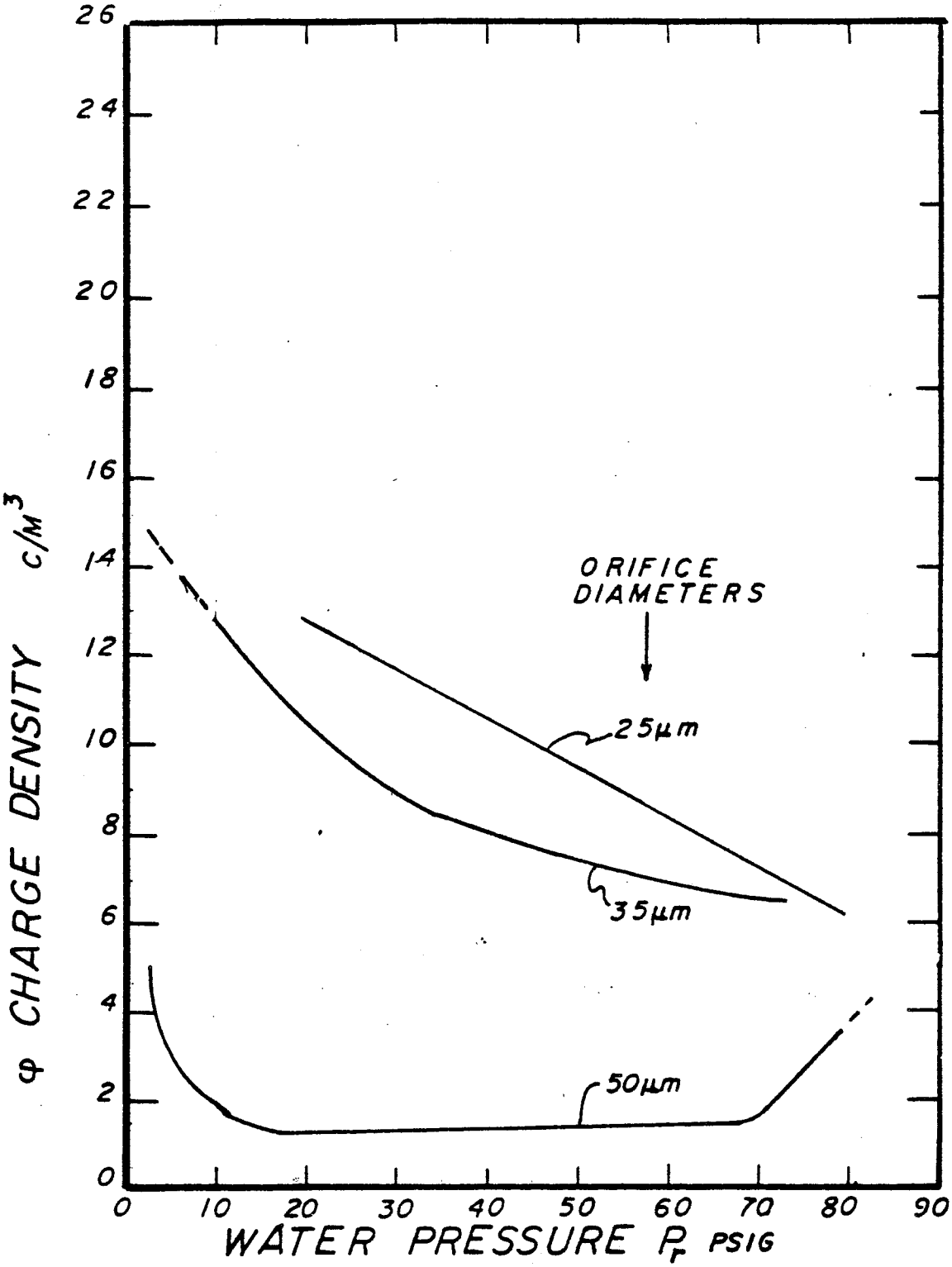

FIG. 22

RELATIONSHIP BETWEEN THE ELECTRIC CHARGE DENSITY
ON THE WATER DROPLET
AND
WATER PRESSURE P_r psig
FOR
VARIOUS PLATE ORIFICES, 25, 35, and 50 μm DIAMETERS
AND
CONSTANT LENGTH 25 μm

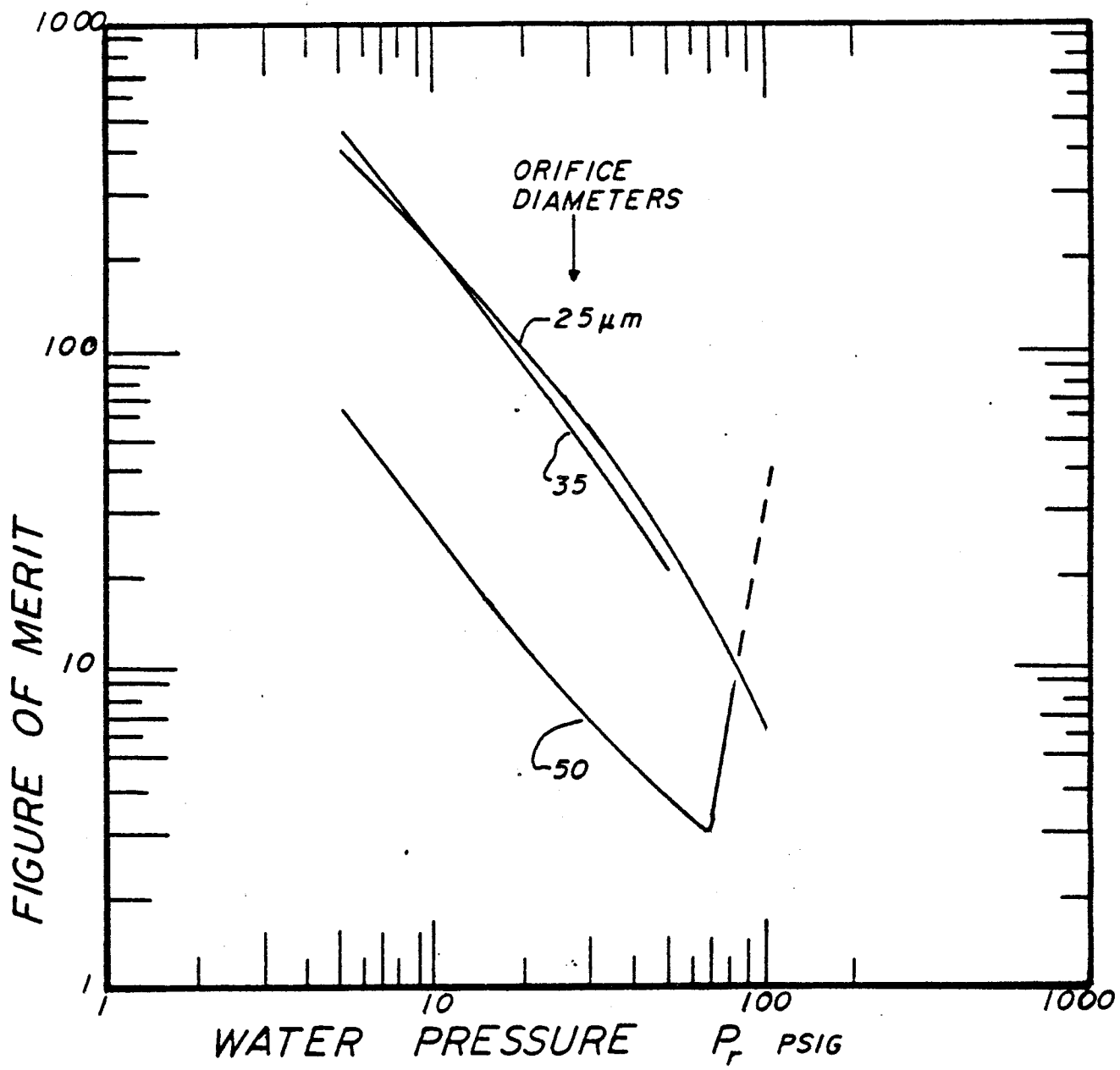

FIG. 23

FIGURE OF MERIT F (μA/Watt)
vs
WATER PRESSURE P_r PSIG
FOR
PLATE ORIFICES HAVING VARIOUS DIAMETERS
25, 35, and 50 μm
FOR
CONSTANT LENGRH 25 μm

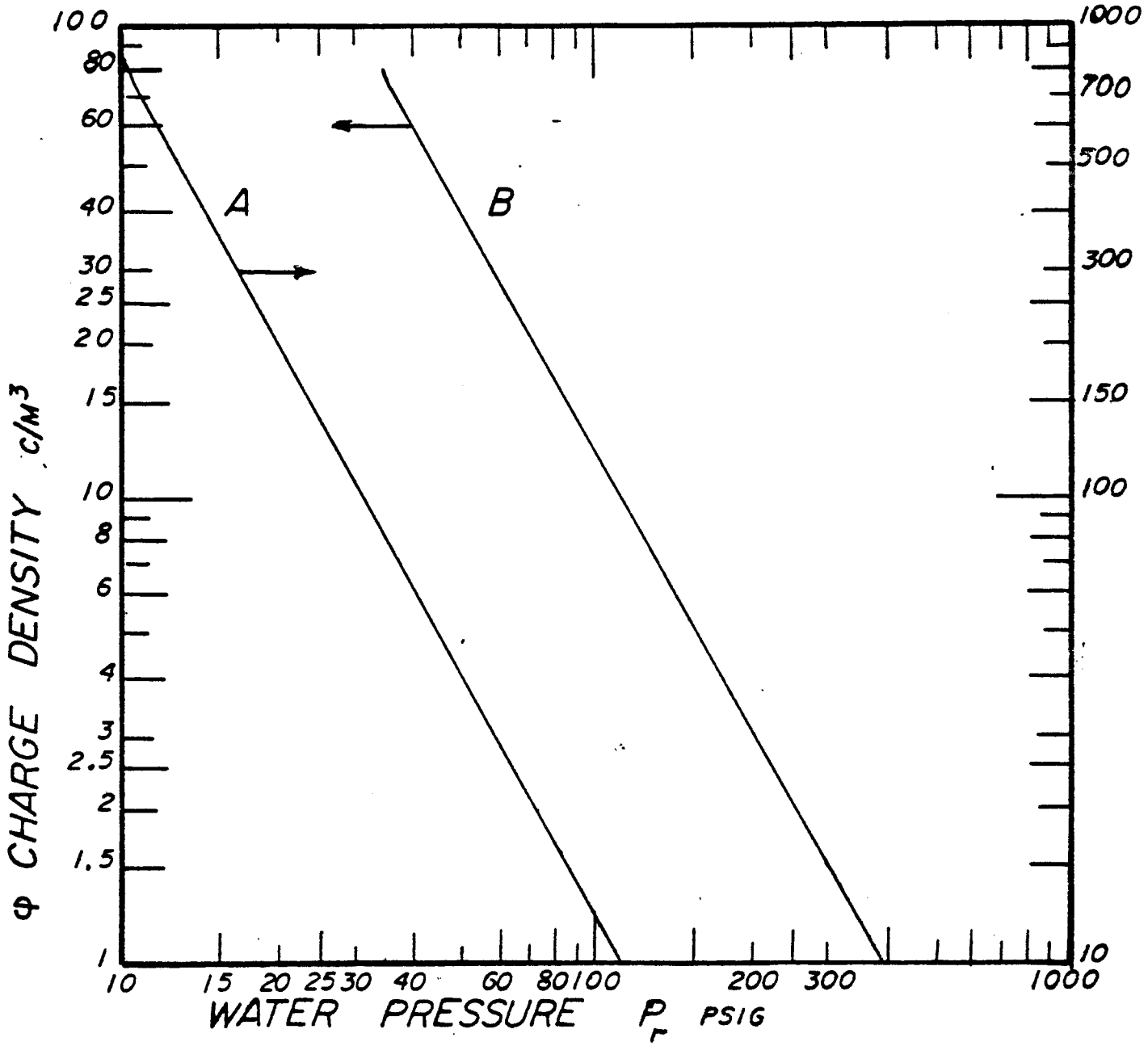

FIG. 24

PLOT OF THEORETICAL EQUATION (61)
SHOWING
ELECTRIC CHARGE DENSITY ON WATER
vs
ORIFICE DIAMETER d_j IN μm

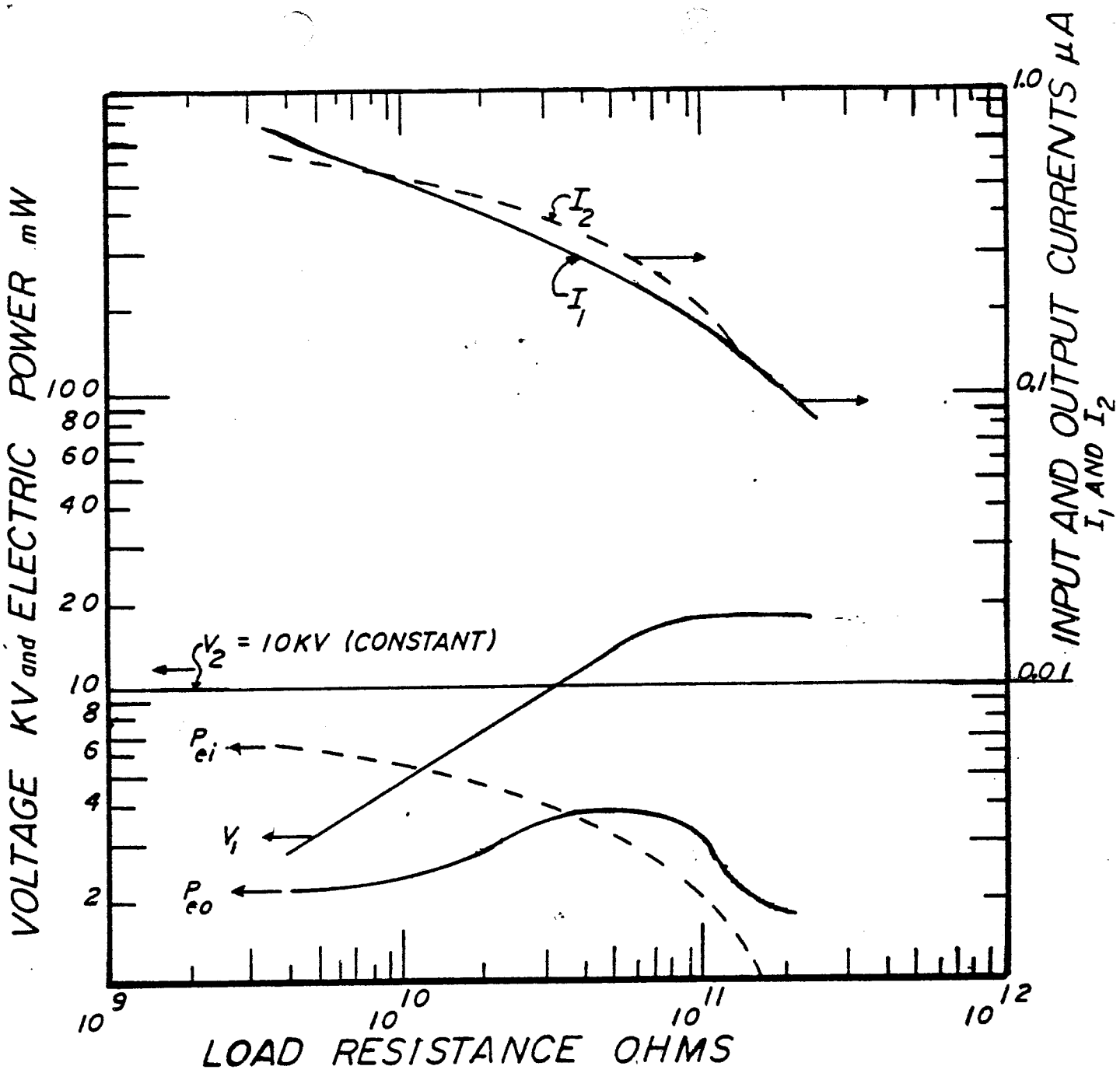

FIG. 25

INPUT AND OUTPUT CURRENTS
AND
INPUT AND OUTPUT VOLTAGES
vs
LOAD RESISTANCE (ohms) FOR THE FOLLOWING CONDITIONS;
d_j = 50 μm, P_r = 50 psig CONSTANT
V_2 = 10kV CONSTANT
EXCITER RING 60 μm DIAMETER
CONSTANT FLOW RATE Q = 4.4 x $10^{-8}m^3/s$
AND
CONSTANT WIND VELOCITY U_w = 7.5m/s

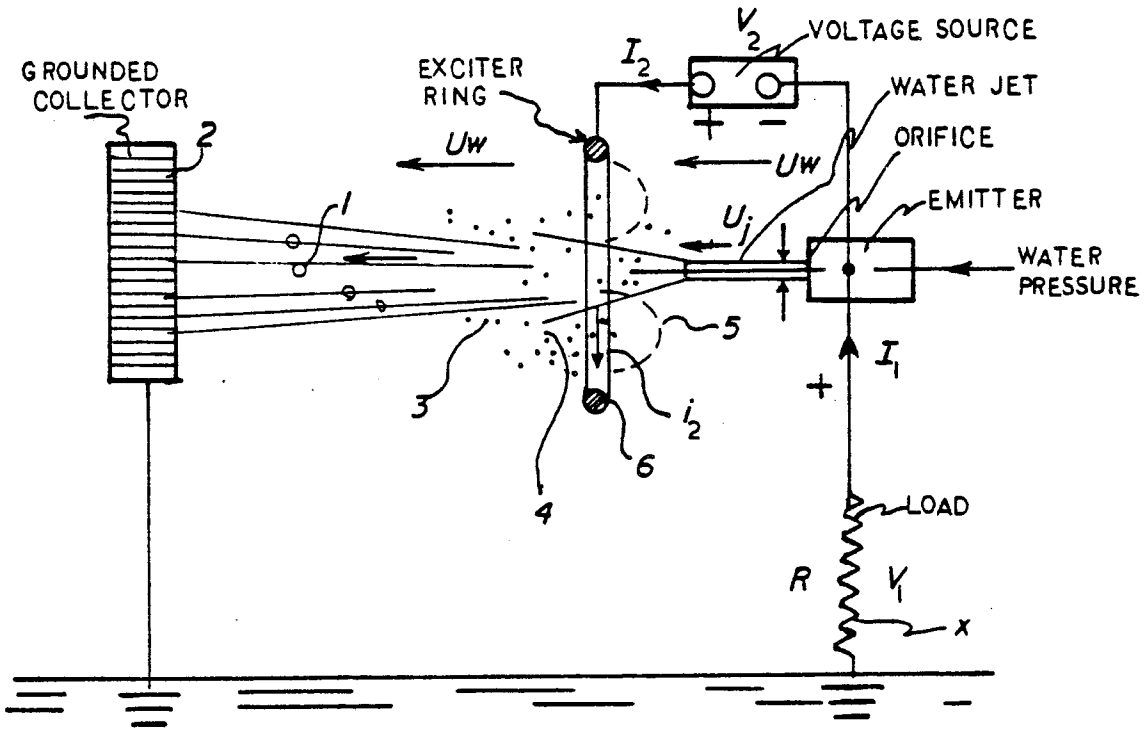

FIG. 26

DIAGRAM OF A WATER JET WITH INDUCTION ELECTRIC CHARGING WITH SELF-LIMITING EXCITER CURRENT DUE TO INCREASING SPACE CHARGE FIELD

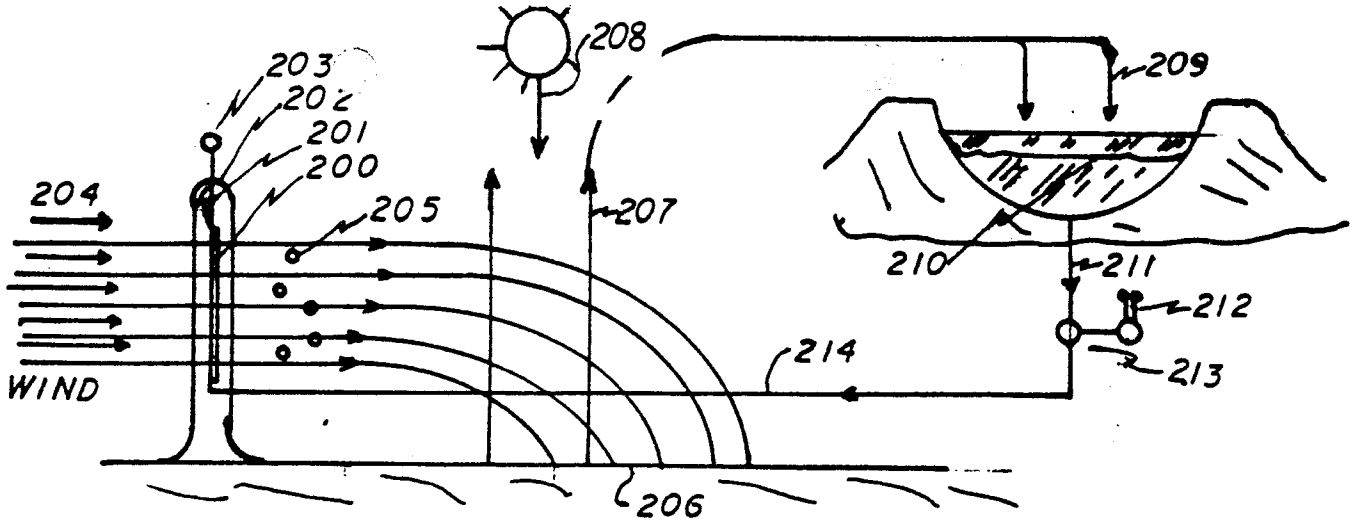

FIG. 27.1

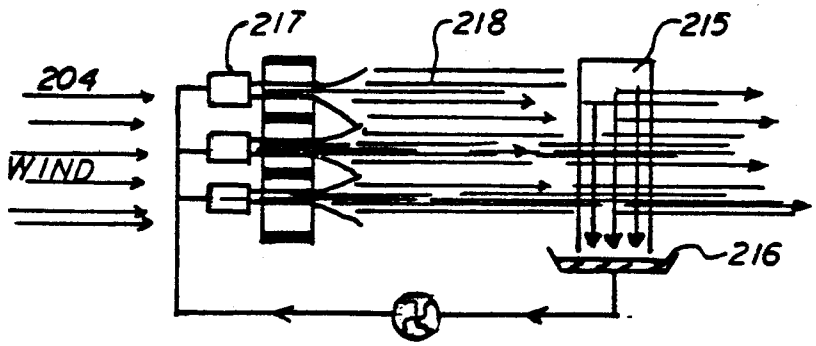

FIG. 27.2

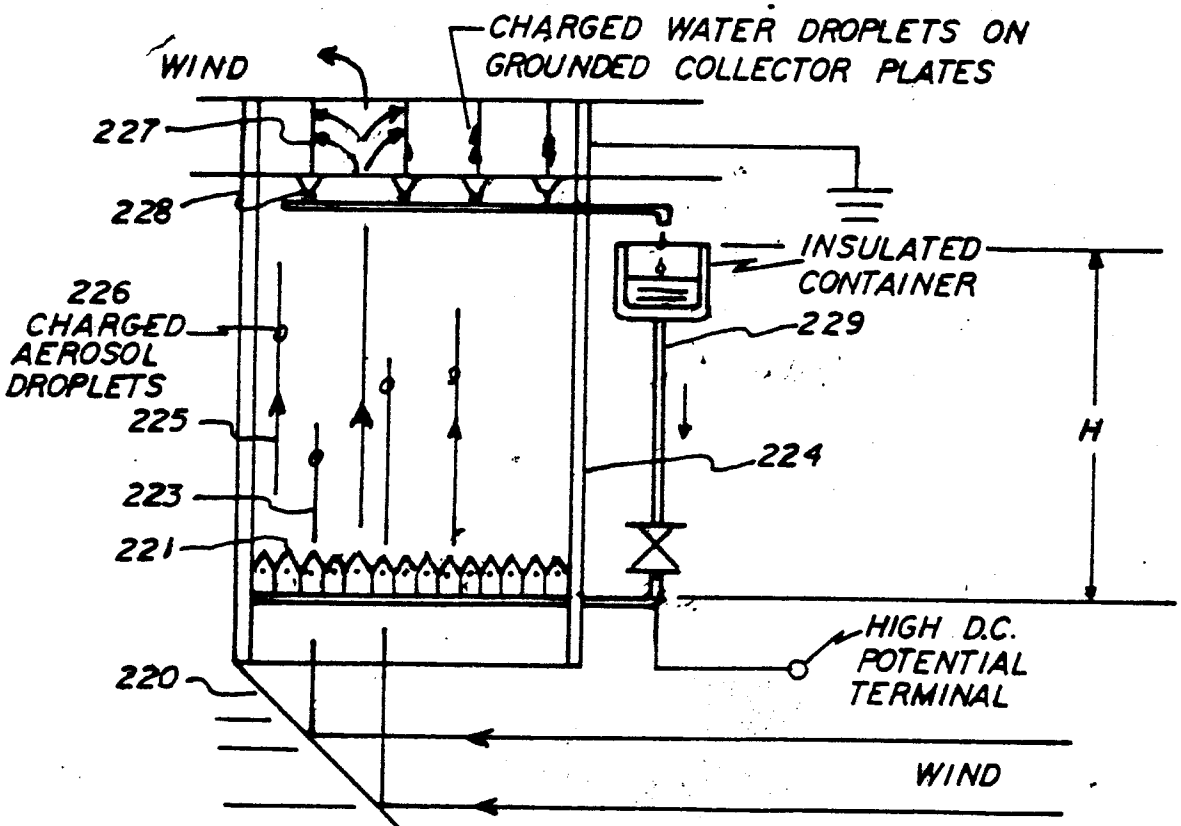

FIG. 27

FIG. 27.3

W/E/P GENERATOR WITH WATER RECUPERATION & PRESSURE REGENERATION

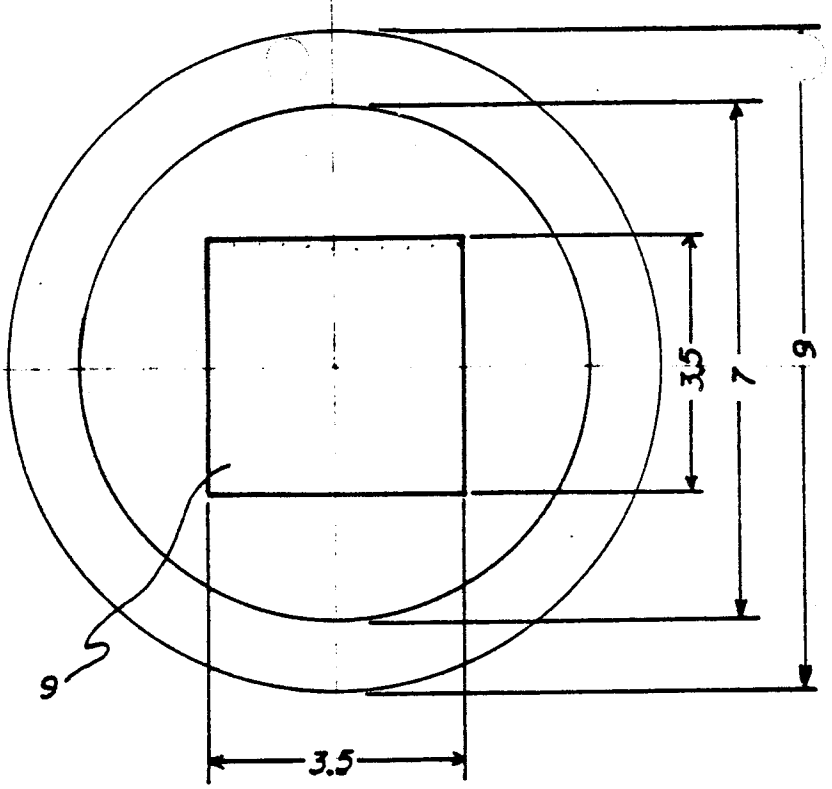

FIG. 28.1

SCALE 10:1

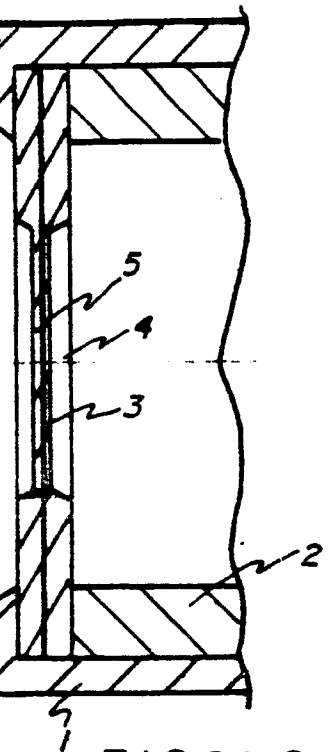

FIG. 28.2

Scale: 10:1

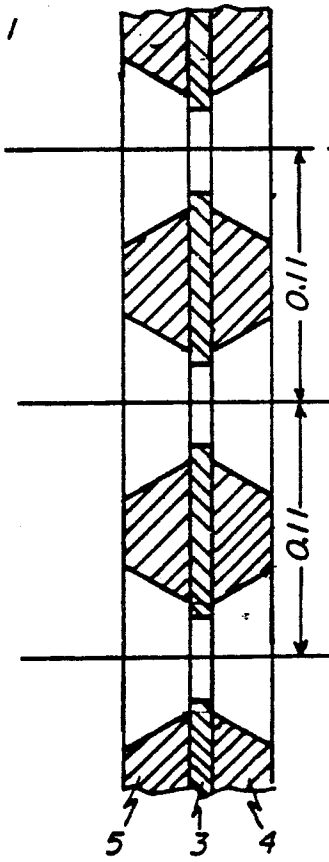

FIG. 28.4

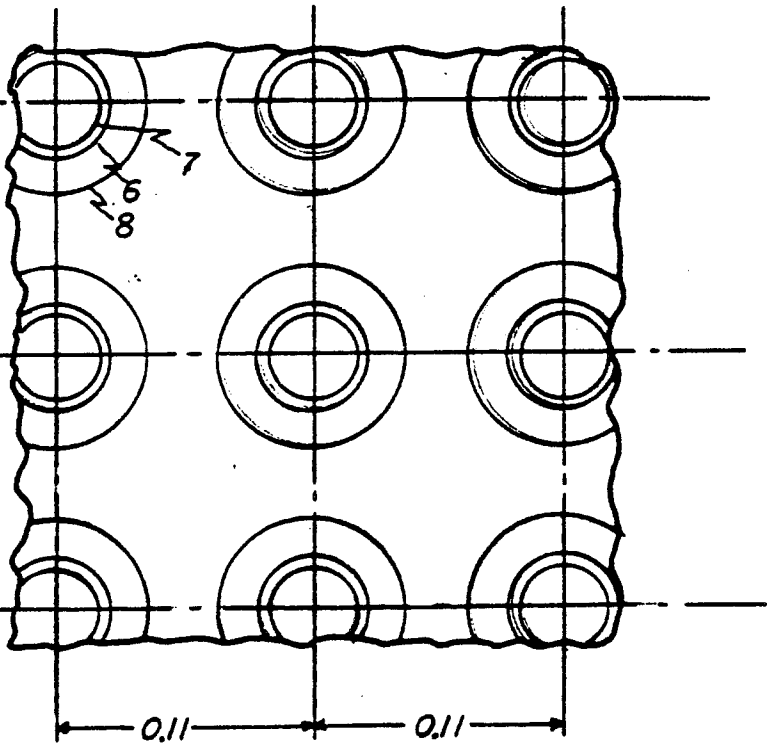

Scale: 320:1

FIG. 28.3

FIG. 28

PLATE ORIFICE ARRAY
32 X 32 = 1024 ORIFICES

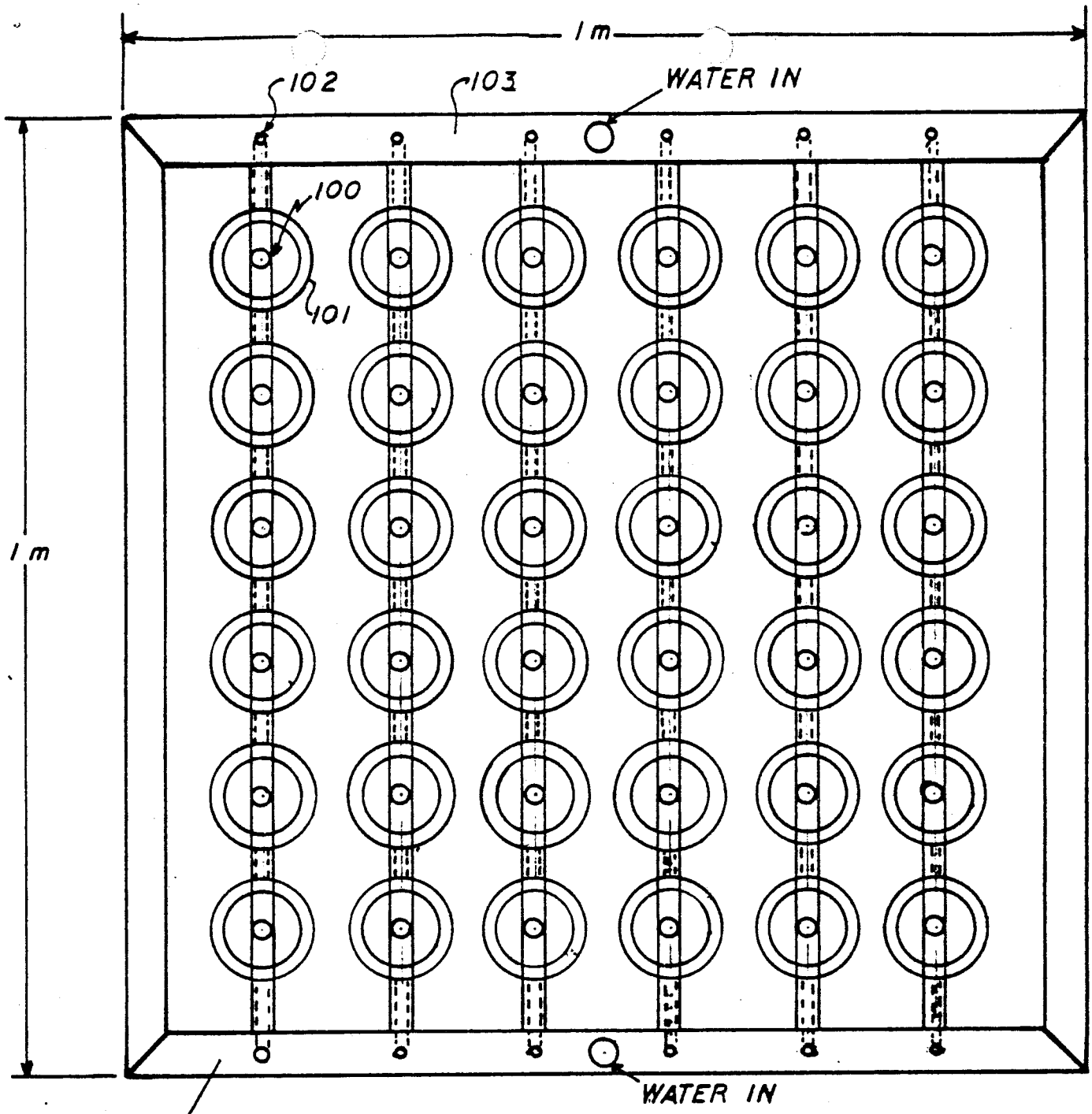

FIG. 29

PLAN VIEW SCHEMATIC
36 = 6 x 6 SUPER ARRAY
32 x 32 = 1024 MULTIORIFICE PLATE ARRAYS
36,864 ORIFICES/m^2

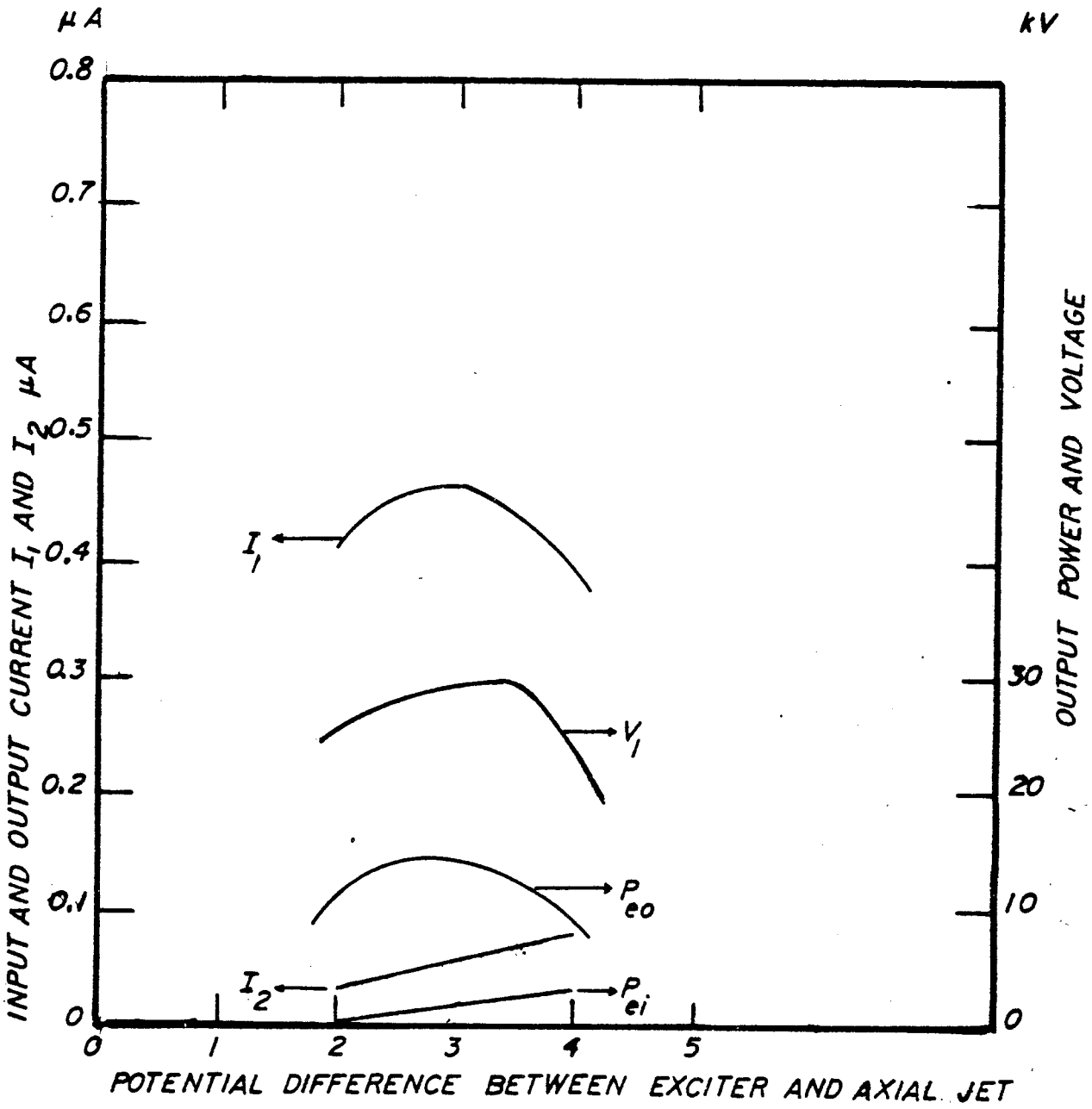

FIG. 30

Input and output currents I_1 and I_2 μA
Output power P_{eo} watts and output voltage V kV
vs
Potential Difference V_2 kV
between
Exciter and Axial jet

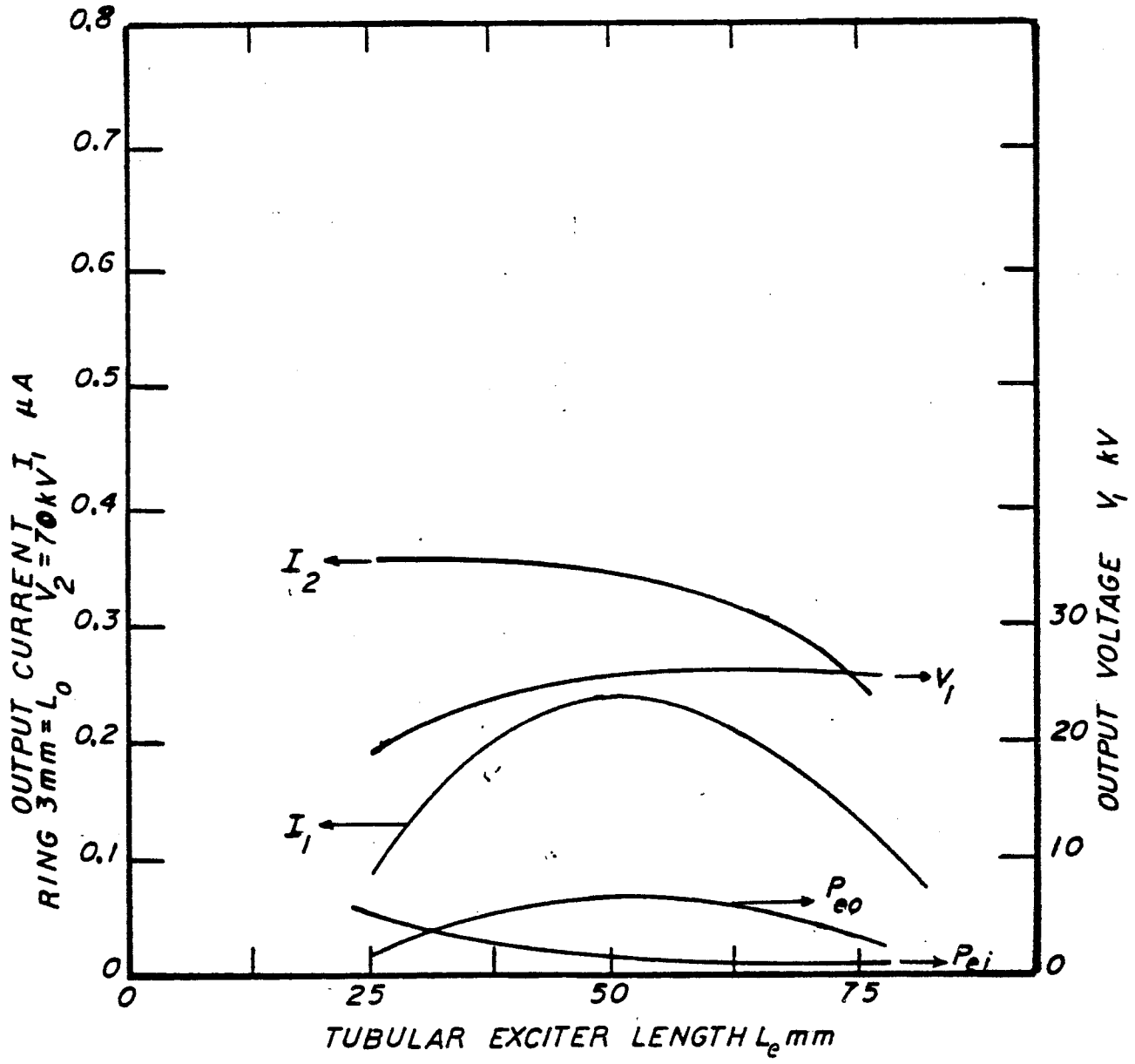

FIG. 31

OUTPUT AND INPUT CURRENTS
AND
I_2 μA VOLTAGE V_1 kV, POWER P_{eo} WATTS
AND
INPUT POWER P_{ei}
vs
TUBULAR EXCITER LENGTH L_e mm

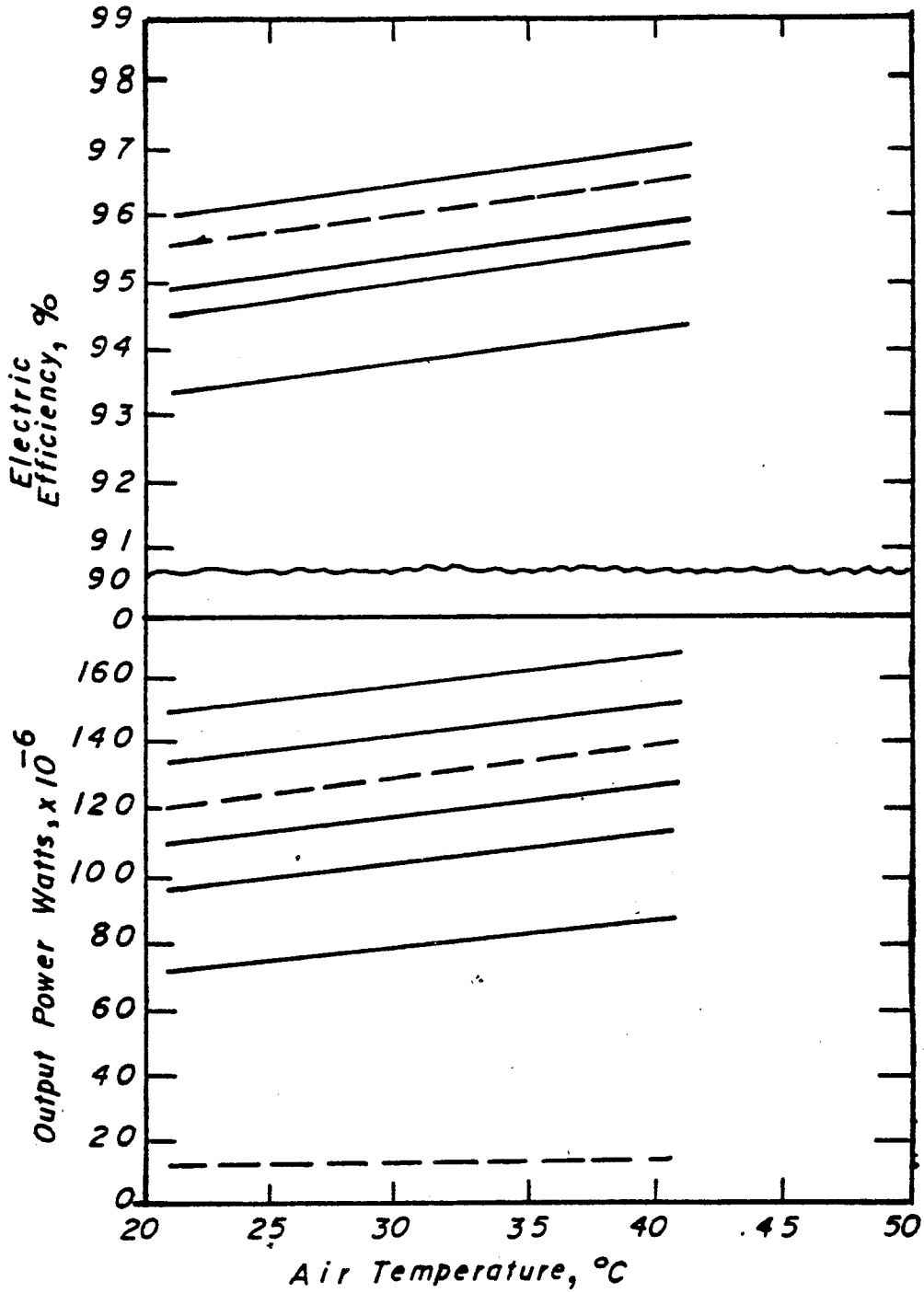

FIG. 32

CONSTANT VOLTAGE V_2 = 4.0kV
POWER OUT AND POWER IN, WATTS X 10^{-6}
vs
TEMPERATURE IN °C AND EFFICIENCY IN % (ELECTRIC)
vs
TEMPERATURE, °C AT RELATIVE HUMIDITY, %RH
WIND VELOCITY CONSTANT AT 10 m/s

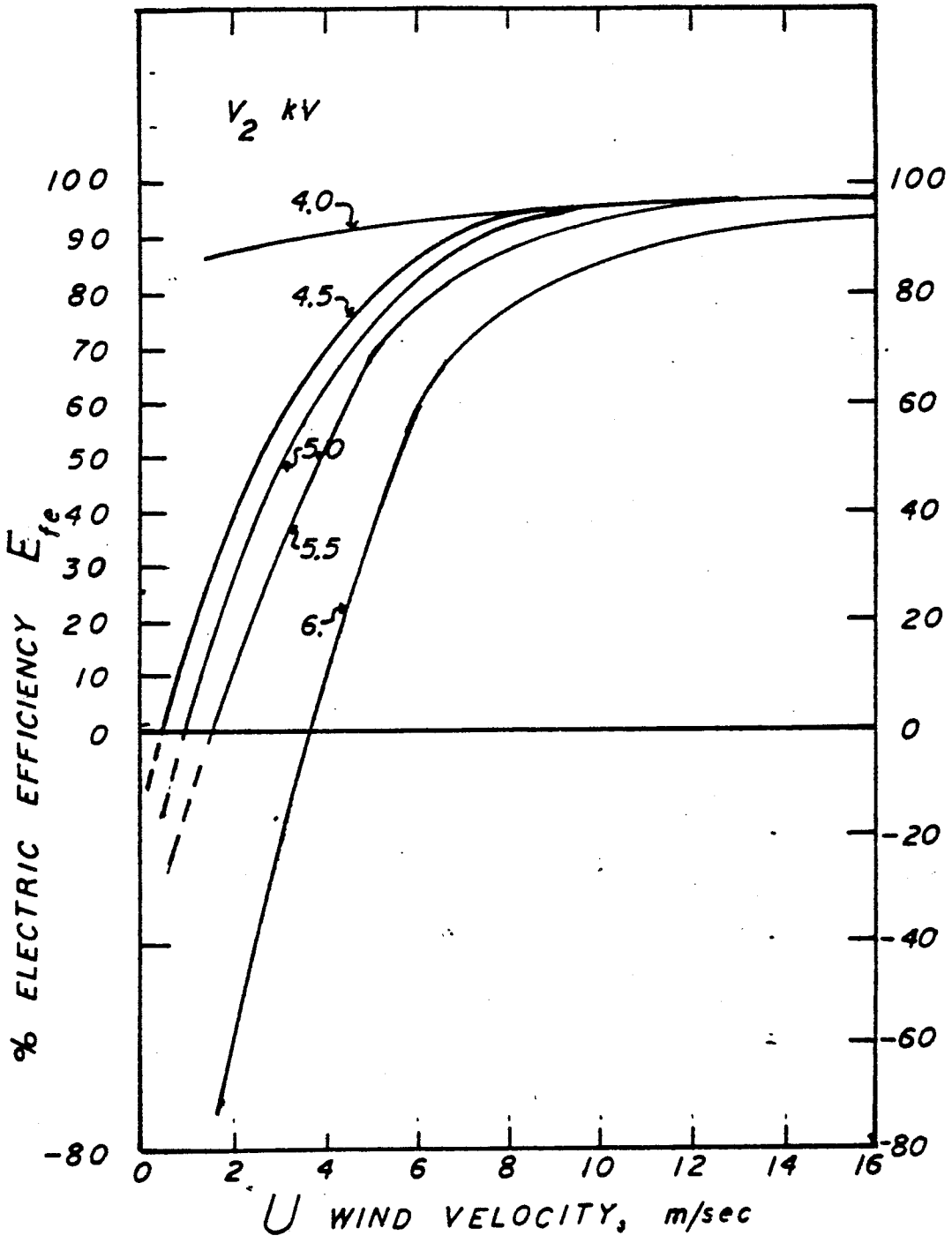

FIG. 33

% EFFICIENCY, ELECTRIC
VS
WIND VELOCITY

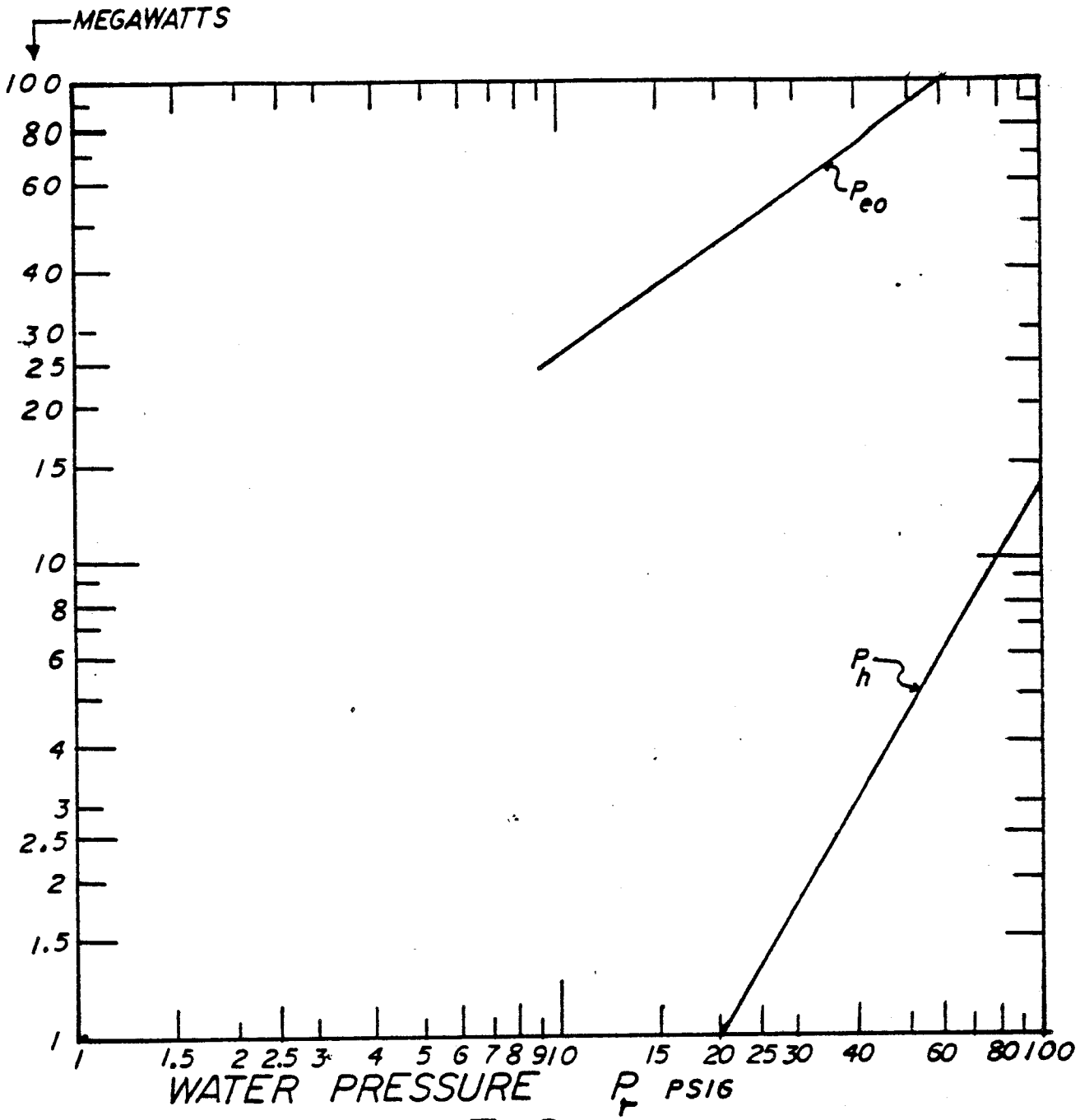

FIG. 34

SHOWING ELECTRIC POWER OUTPUT
vs
HYDRAULIC OUTPUT SCALED TO MULTI-MEGAWATT OUTPUT
USING

$10^5 M^2$ AND SUPER ARRAYS OR MULTI-ARRAYS
EACH
35 μm DIAMETER
AND
25 μm LONG